

JET PROPULSION LABORATORY

SIRTF IPF REPORT

JPL ID502087

November 20, 2003

**SIRTF INSTRUMENT POINTING FRAME  
KALMAN FILTER EXECUTION SUMMARY**

IPF RUN NUMBER: 502087

REPORT TYPE: IOC EXECUTION (FINE)

PRIME FRAME: MIPS\_160um\_center\_large\_FOV (87)

INFERRRED FRAMES: (88) (89) (91) (92)

**IPF TEAM**

Autonomy and Control Section (345)

Jet Propulsion Laboratory

California Institute of Technology

4800 Oak Grove Drive

Pasadena, CA 91109

# Contents

<b>1 IPF EXECUTION SUMMARY</b>	<b>5</b>
<b>2 IPF INPUT FILE HISTORY</b>	<b>9</b>
<b>3 IPF EXECUTION RESULTS</b>	<b>13</b>
3.1 IPF EXECUTION OUTPUT PLOTS . . . . .	13
3.2 IPF OUTPUT DATA (IF MINI FILE) . . . . .	39
3.3 IPF EXECUTION LOG . . . . .	42
<b>4 COMMENTS</b>	<b>46</b>

## List of Figures

1.1 A-priori and a-posteriori IPF frames . . . . .	5
1.2 A-priori and a-posteriori IPF frames (ZOOMED) . . . . .	8
2.1 Scenario Plot . . . . .	9
2.2 Attitude file edit history . . . . .	10
2.3 Centroid file edit history . . . . .	11
2.4 Oriented Pixel Coords of Centroid Meas. Edited Centroids . . . . .	12
3.1 TPF coords of measurements and a-priori predicts . . . . .	15
3.2 Oriented Pixel Coords of measurements and a-priori predicts . . . . .	15
3.3 Oriented (W,V) Pixel Coords of A-Priori Prediction Error Quiver Plot . . . . .	16
3.4 A-priori prediction error (Science Centroids) . . . . .	16
3.5 Oriented Pixel Coords of measurements and a-priori predicts (PCRS only) . . . . .	17
3.6 Oriented Pixel Coords of measurements and a-priori predicts (Zoomed, PCRS only)	17
3.7 Oriented (W,V) Pixel Coords of A-Priori PCRS Prediction Error Quiver Plot . . . . .	18
3.8 A-priori PCRS prediction error . . . . .	18
3.9 IPF execution convergence, chart 1 . . . . .	19
3.10 IPF execution convergence, chart 2 . . . . .	19
3.11 Parameter uncertainty convergence . . . . .	20
3.12 IPF parameter symbol table . . . . .	20

3.13 KF parameter error sigma plots . . . . .	21
3.14 LS parameter error sigma plot . . . . .	21
3.15 KF and LS parameter error sigma plot . . . . .	22
3.16 Oriented Pixel Coords of meas. and a-posteriori predicts . . . . .	23
3.17 Oriented Pixel Coords of meas. and a-posteriori predicts (attitude corrected) . . . . .	23
3.18 KF innovations with (o) and w/o (+) attitude corrections . . . . .	24
3.19 Histograms of science a-posteriori residuals (or innovations) . . . . .	24
3.20 A-Posteriori Science Centroid Prediction Error Quiver (Att. Cor.) . . . . .	25
3.21 Normalized A-Posteriori Science Centroid Prediction Errors . . . . .	25
3.22 KF innovations with (o) and w/o (+) attitude corrections (PCRS) . . . . .	26
3.23 Histograms of PCRS a-posteriori residuals (or innovations) . . . . .	26
3.24 A-posteriori PCRS Prediction Summary . . . . .	27
3.25 A-posteriori PCRS Prediction (PCRS 1 Only) . . . . .	28
3.26 A-posteriori PCRS Prediction (PCRS 2 Only) . . . . .	28
3.27 A-Posteriori PCRS Prediction Errors Quiver (Att. Cor.) . . . . .	29
3.28 Normalized A-Posteriori PCRS Prediction Errors . . . . .	29
3.29 W-axis KF innovations and 1-sigma bound . . . . .	30
3.30 V-axis KF innovations and 1-sigma bound . . . . .	30
3.31 Array plot with (solid) and w/o (dashed) optical distortion corrections . . . . .	31
3.32 Optical Distortion Plot: total (x5 magnification) . . . . .	31
3.33 Optical Distortion Plot: constant plate scales (x5 magnification) . . . . .	32
3.34 Optical Distortion Plot: linear plate scale (x5 magnification) . . . . .	32
3.35 Optical Distortion Plot: gamma terms (x5 magnification) . . . . .	33
3.36 Scan Mirror Chops . . . . .	33
3.37 IPF Frame Reconstruction . . . . .	34
3.38 Center Pixel Reconstruction . . . . .	34
3.39 Estimated attitude corrections (Body frame) . . . . .	35
3.40 Estimated attitude error sigma plot (Body frame) . . . . .	35
3.41 Thermo-mechanical boresight drift (equiv. angle in (W,V) coords) . . . . .	36
3.42 Thermo-mechanical boresight drift (equiv. angle in Body frame) . . . . .	36
3.43 Gyro drift bias contribution (equiv. rate in (W,V) coords) . . . . .	37

3.44	Gyro drift bias contribution (equiv. angle in (W,V) coords)	37
3.45	Gyro drift bias contribution (equiv. angle in Body frame)	38

## List of Tables

1.1	IPF filter input files	6
1.2	IPF filter execution configuration	6
1.3	IPF filter execution mask vector assignment	6
1.4	IPF calibration error summary ([arcsec], 1-sigma, radial)	7
1.5	Science measurement prediction error summary (1-sigma)	7
1.6	IPF Brown angle summary	8
2.1	IPF input file begin and end times	9
2.2	IPF input file editing status	9
2.3	List of Removed Centroids (Original CA File Row Index)	12
2.4	List of Removed PCRS Centroids (Original CB File Row Index)	12
3.1	Table of figures I (IPF run)	13
3.2	Table of figures II (IPF run)	14
3.3	PCRS measurement prediction error summary	27

# 1 IPF EXECUTION SUMMARY

This report summarizes the SIRTF Instrument Pointing Frame (IPF) Kalman Filter execution associated with run file: RN502087. In particular, this Focal Point Survey calibrates the instrument: MIPS\_160um\_center\_large\_FOV (87), as part of the IOC Fine Survey. The main calibration results from the IPF filter execution have been documented in IF502087 typically stored in the mission archive DOM collection IPF\_IF. This report only summarizes the main aspects of the run, and does not substitute for the full information contained in the IF file.

Section 1 summarizes the filter execution results. The filter configurations are tabulated in Table 1.2 and the mask vector assignments are tabulated in Table 1.3. A total of 17 state parameters are estimated in this run. The overall End-to-End pointing performances are tabulated in Table 1.4. The prediction residuals throughout the estimation processes are tabulated in Table 1.5. Section 3 summarizes resulting plots, a mini summary of the IF IPF output file, and the execution log. Section 4 captures the user comments that are specific to this particular run.

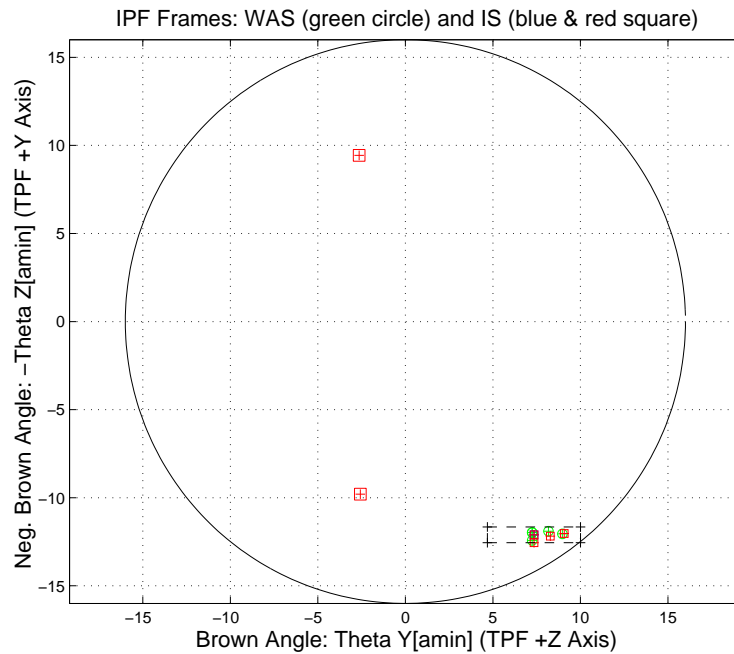


Figure 1.1: A-priori and a-posteriori IPF frames

RAW	FINAL (After Editing)
AA501087	AA501087
AS501087	AS501087
CA501087	CA902087
CB502087	CB901087
CS501087	CS501087

Table 1.1: IPF filter input files

EXECUTION CONFIGURATION ITEM	CURRENT STATUS
IPF Filter Version Used	IPF.V3.0.0B
Frame Table Version Used	BodyFrames_FTU_13Aa
Scan-Mirror Employed?	NO
IPF Filter Mode	NORMAL-MODE(0)
SLIT-MODE Operation	DISABLED
Kalman Filter Operation	ENABLED
Least-Squares Data Analysis	ENABLED
IBAD Screening	DISABLED
User-Specified Data Editing	DISABLED
Total Number of Iterations	30
LS Residual Sigma Scale	9.07080316E-001
Total Number of Maneuvers	29

Table 1.2: IPF filter execution configuration

Con. Plate Scale			$\Gamma$ Dependent				$\Gamma^2$ Dependent				Linear Plate Scale						Mirror	
$a_{00}$	$b_{00}$	$c_{00}$	$a_{10}$	$b_{10}$	$c_{10}$	$d_{10}$	$a_{20}$	$b_{20}$	$c_{20}$	$d_{20}$	$a_{01}$	$b_{01}$	$c_{01}$	$d_{01}$	$e_{01}$	$f_{01}$	$\alpha$	$\beta$
1	2	3	4	5	6	7	8	9	10	11	12	13	14	15	16	17	18	19
0	0	0	0	0	0	0	0	0	0	0	0	0	0	0	0	0	0	0
IPF (T)			Alignment R						Gyro Drift Bias									
$\theta_1$	$\theta_2$	$\theta_3$	$a_{rx}$	$a_{ry}$	$a_{rz}$	$b_{rx}$	$b_{ry}$	$b_{rz}$	$c_{rx}$	$c_{ry}$	$c_{rz}$	$b_{gx}$	$b_{gy}$	$b_{gz}$	$c_{gx}$	$c_{gy}$	$c_{gz}$	
20	21	22	23	24	25	26	27	28	29	30	31	32	33	34	35	36	37	
0	1	1	1	1	1	1	1	1	1	1	1	1	1	1	1	1	1	

Table 1.3: IPF filter execution mask vector assignment

**FOCAL PLANE SURVEY ANALYSIS: IOC Fine Survey.**

**INSTRUMENT NAME: MIPS\_160um\_center\_large\_FOV NF: 87**

**PIX2RADW: 7.73998982E-005 [rad/pixel] = 1.5965E+001 [arcsec/pixel]**

**PIX2RADV: 8.70861410E-005 [rad/pixel] = 1.7963E+001 [arcsec/pixel]**

FRAME	DESCRIPTION	IPF <sup>1</sup>	SF <sup>2</sup>	TOTAL	REQ
087(P)	MIPS_160um_center_large_FOV	0.6195	0.0855	0.6254	3.70
088(I)	MIPS_160um_plusY_edge	0.6195	0.0855	0.6254	N/A
089(I)	MIPS_160um_large_only	0.6195	0.0855	0.6254	N/A
091(I)	MIPS_160um_small_FOV1	0.6195	0.0855	0.6254	N/A
092(I)	MIPS_160um_small_FOV2	0.6195	0.0855	0.6254	N/A

Table 1.4: IPF calibration error summary ([arcsec], 1-sigma, radial)

RMS METRIC	A PRIORI <sup>3</sup>	A POSTERIORI <sup>3</sup>	ATT. CORRECTED <sup>4</sup>	UNITS
Radial	15.8650	16.4352	16.4422	arcsec
W-Axis	8.1779	7.0241	7.0248	arcsec
V-Axis	13.5948	14.8586	14.8660	arcsec
Radial	0.9139	0.9369	0.9373	pixels
W-Axis	0.5122	0.4400	0.4400	pixels
V-Axis	0.7568	0.8272	0.8276	pixels

Table 1.5: Science measurement prediction error summary (1-sigma)

---

<sup>1</sup>IPF filter removes systematic pointing errors due to: thermomechanical alignment drift (Body to TPF), gyro bias and bias drift, centroiding error, attitude error, and optical distortion. IPF SIGMA presented here is “Scaled” by the Least Squares Scale factor. The Least Squares Scale Factor was: 0.907080. It is assumed that the gyro Angle Random Walk contribution is captured with the Least Squares scaling. The gyro ARW contribution can be approximately calculated as 0.0330 arcseconds, given that ARW = 100  $\mu\text{deg}/\sqrt{\text{hr}}$ , with 5.885000e+002 second Maneuver time (max), and 29 independent Maneuvres.

<sup>2</sup>Gyro Scale Factor(GSF) assumes 95 ppm error over 0.250 degree maneuver.

<sup>3</sup>This can be interpreted as estimate of ”pixel to sky” pointing reconstruction error if no science data is used.

<sup>4</sup>This can be interpreted as estimate of achieved S/I centroiding error

IPF BROWN ANGLE SUMMARY					
FRAME TABLE USED: BodyFrames_FTU_13Aa					
NF	NAME	WAS	IS	CHANGE	UNIT
087	theta_Y	+7.240265	+7.347515	+0.107249	arcmin
087	theta_Z	+11.975320	+12.105588	+0.130267	arcmin
087	angle	+0.000002	+0.000006	+0.000005	deg
088	theta_Y	+7.240265	+7.347515	+0.107249	arcmin
088	theta_Z	+12.424391	+12.554659	+0.130267	arcmin
088	angle	+0.000002	+0.000006	+0.000005	deg
089	theta_Y	+7.240265	+7.347515	+0.107249	arcmin
089	theta_Z	+11.975320	+12.105588	+0.130267	arcmin
089	angle	+0.000002	+0.000006	+0.000005	deg
091	theta_Y	+8.969800	+9.077043	+0.107243	arcmin
091	theta_Z	+12.050100	+12.030743	-0.019357	arcmin
091	angle	+0.000000	+0.000006	+0.000006	deg
092	theta_Y	+8.171600	+8.278799	+0.107199	arcmin
092	theta_Z	+11.900500	+12.180433	+0.279933	arcmin
092	angle	-0.000000	+0.000006	+0.000006	deg

Table 1.6: IPF Brown angle summary

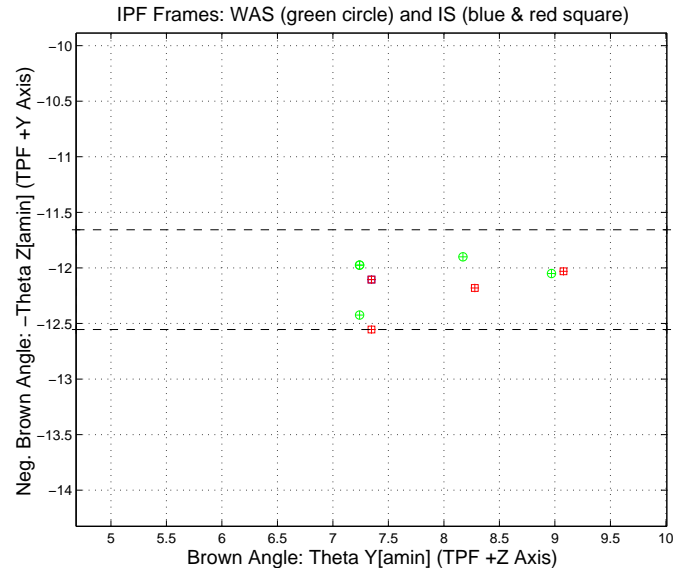


Figure 1.2: A-priori and a-posteriori IPF frames (ZOOMED)

## 2 IPF INPUT FILE HISTORY

STATUS	FILENAME	START TIME	END TIME
WAS	AA501087	752744000.3	752773000.4
IS	AA501087	752744000.3	752773000.4
WAS	CA501087	752745107.5	752772166.5
IS	CA902087	752745107.5	752772166.5
WAS	CB502087	752744913.3	752772305.4
IS	CB901087	752744913.3	752772305.4

Table 2.1: IPF input file begin and end times

WAS	SIZE	IS	SIZE	REMOVED	PATCHED
AA501087	290002	AA501087	290002	0	0
CA501087	332	CA902087	322	10	N/A
CB502087	180	CB901087	178	2	N/A

Table 2.2: IPF input file editing status

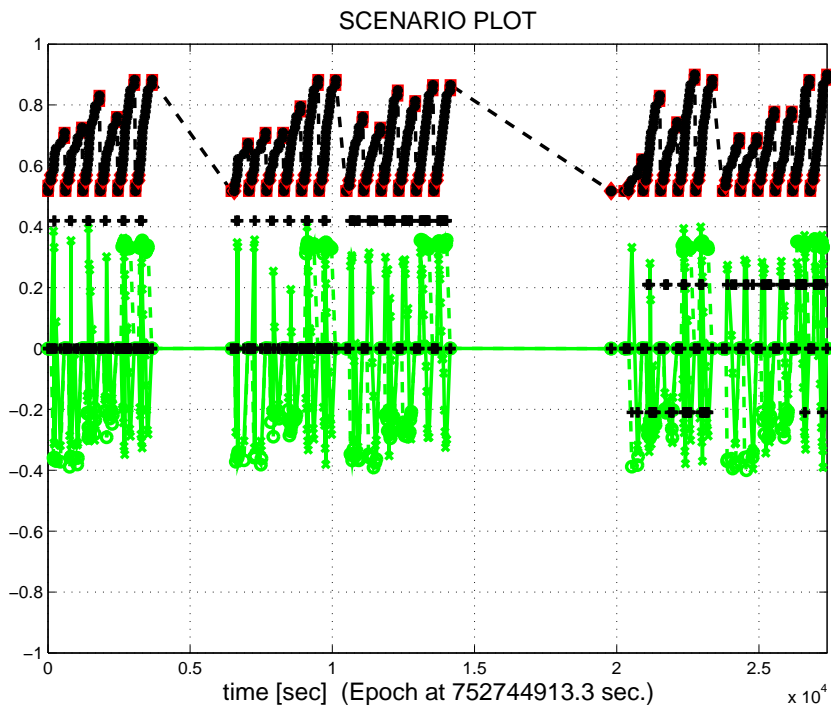


Figure 2.1: Scenario Plot

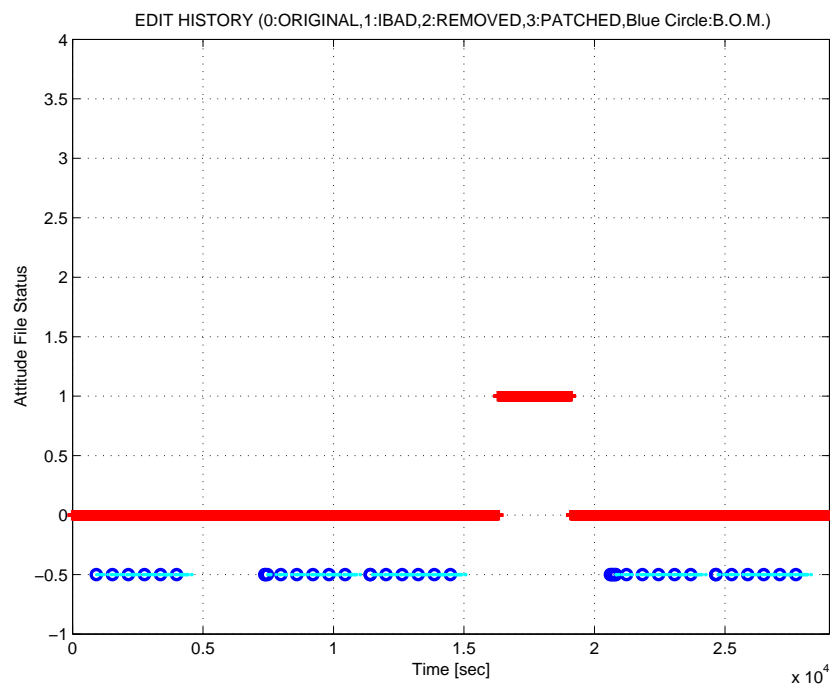


Figure 2.2: Attitude file edit history

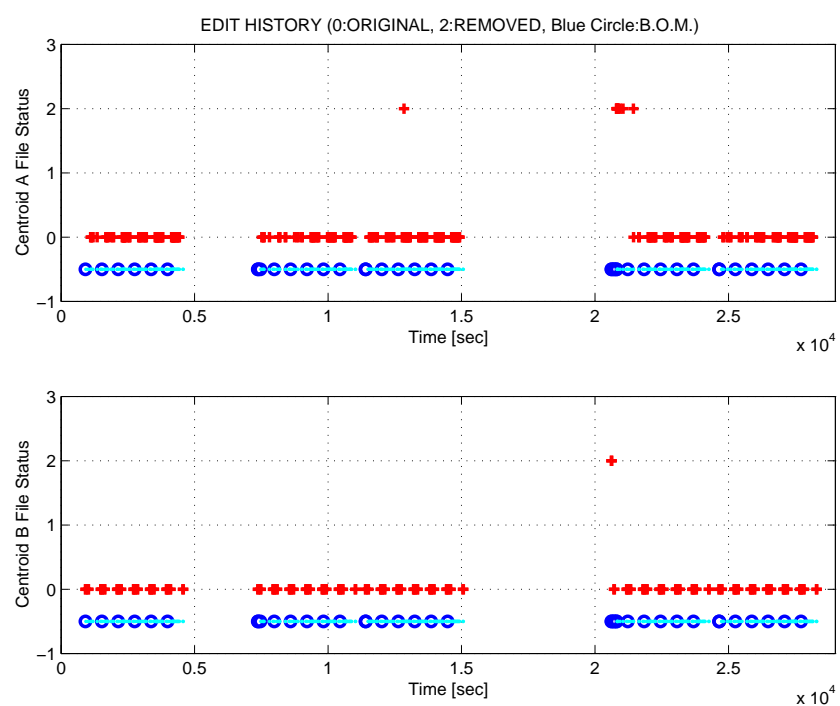


Figure 2.3: Centroid file edit history

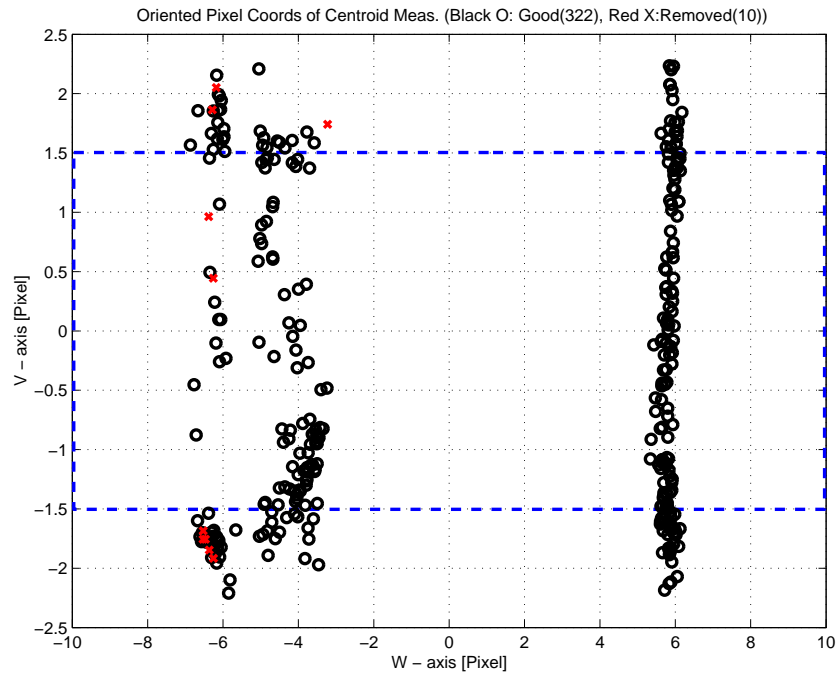


Figure 2.4: Oriented Pixel Coords of Centroid Meas. Edited Centroids

LIST OF REMOVED SCIENCE CENTROIDS									
149	203	204	205	206	207	208	209	210	211

Table 2.3: List of Removed Centroids (Original CA File Row Index)

LIST OF REMOVED PCRS CENTROIDS									
109	110								

Table 2.4: List of Removed PCRS Centroids (Original CB File Row Index)

### 3 IPF EXECUTION RESULTS

#### 3.1 IPF EXECUTION OUTPUT PLOTS

This subsection summarizes the IPF filter results. As shown in Table 3.1, the output plots are segmented to three groups: predicted performance, post-run results and IPF trending plots.

FIGURE NO.	DESCRIPTION
<b>Predicted performance prior to IPF run</b>	
Figure 3.1	Meas. and a-priori predicts in TPF coords
Figure 3.2	Meas. and a-priori predicts in Oriented Pixel Coords including rectangular array boundary approximation
Figure 3.3	A-Priori Prediction Error Quiver Plot in Oriented Pixel Coords including rectangular array boundary approximation
Figure 3.4	A-priori prediction error
Figure 3.5	Oriented Pixel Coords of measurements and a-priori predicts (PCRS only)
Figure 3.6	Oriented Pixel Coords of measurements and a-priori predicts (Zoomed, PCRS only)
Figure 3.7	Oriented (W,V) Pixel Coords of A-Priori PCRS Prediction Error Quiver Plot
Figure 3.8	A-priori PCRS prediction error
<b>IPF filter performance (post run results)</b>	
Figure 3.9	IPF execution convergence, chart 1: (top) normalized residual error vs. iteration number and (bottom) norm of effective parameter corrections
Figure 3.10	IPF execution convergence, chart 2: parameter correction size vs. iteration number
Figure 3.11	Parameter uncertainty convergence: square-root of diagonal elements of covariance matrix vs. maneuver number
Figure 3.12	IPF parameter symbol table
Figure 3.13	KF parameter error sigma plot (a-priori-dashed, a-posteriori-solid). Includes true parameter errors (FLUTE runs only)
Figure 3.14	LS parameter error sigma plot. Includes true parameter errors (FLUTE runs only)
Figure 3.15	KF and LS parameter errors sigma plot (Figure 3.13 & Figure 3.14 combined)
Figure 3.16	Measurements and a-posteriori predicts in Oriented Pixel Coords including rectangular array boundaries (a-priori-dashed, a-posteriori-solid)
Figure 3.17	Attitude corrected meas. and a-posteriori predicts in Oriented Pixel Coords including rectangular array boundaries (a-priori-dashed, a-posteriori-solid)

Table 3.1: Table of figures I (IPF run)

FIGURE NO.	DESCRIPTION
<b>IPF filter performance (post run results) - CONTINUE</b>	
Figure 3.18	KF innovations with (o) and w/o (+) attitude corrections
Figure 3.19	Histograms of science a-posteriori residuals (or innovations)
Figure 3.20	A-Posteriori Science Centroid Prediction Error Quiver (Att. Cor.)
Figure 3.21	Normalized A-Posteriori Science Centroid Prediction Errors
Figure 3.22	KF innovations with (o) and w/o (+) attitude corrections (PCRS)
Figure 3.23	Histograms of PCRS a-posteriori residuals (or innovations)
Figure 3.24	A-posteriori PCRS Prediction Summary
Figure 3.25	A-posteriori PCRS Prediction (PCRS 1 Only)
Figure 3.26	A-posteriori PCRS Prediction (PCRS 2 Only)
Figure 3.27	A-Posteriori PCRS Prediction Errors Quiver (Att. Cor.)
Figure 3.28	Normalized A-Posteriori PCRS Prediction Errors
Figure 3.29	W-axis KF innovations and 1-sigma bound
Figure 3.30	V-axis KF innovations and 1-sigma bound
Figure 3.31	Array plot with (solid) and w/o (dashed) optical distortion corrections
Figure 3.32	Optical Distortion Plot: total (x5 magnification)
Figure 3.33	Optical Distortion Plot: constant plate scales (x5 magnification)
Figure 3.34	Optical Distortion Plot: linear plate scale (x5 magnification)
Figure 3.35	Optical Distortion Plot: gamma terms (x5 magnification)
Figure 3.36	Scan Mirror Chops
Figure 3.37	IPF Frame Reconstruction
Figure 3.38	Center Pixel Reconstruction
<b>IPF parameter trending plots</b>	
Figure 3.39	Estimated attitude corrections (Body frame)
Figure 3.40	Estimated attitude error sigma plot (Body frame)
Figure 3.41	Systematic error attributed to thermo-mechanical boresight drift (equiv. angle in (W,V) coords)
Figure 3.42	Systematic error attributed to thermo-mechanical boresight drift (equiv. angle in Body frame)
Figure 3.43	Systematic error attributed to gyro drift bias (equiv. rate in (W,V) coords)
Figure 3.44	Systematic error attributed to gyro drift bias (equiv. angle in (W,V) coords)
Figure 3.45	Systematic error attributed to gyro drift bias (equiv. angle in Body frame)

Table 3.2: Table of figures II (IPF run)

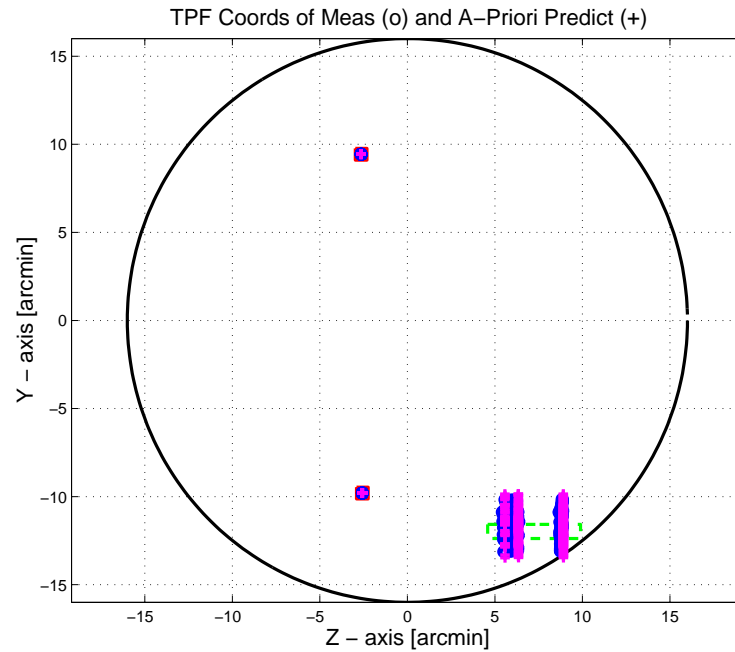


Figure 3.1: TPF coords of measurements and a-priori predicts

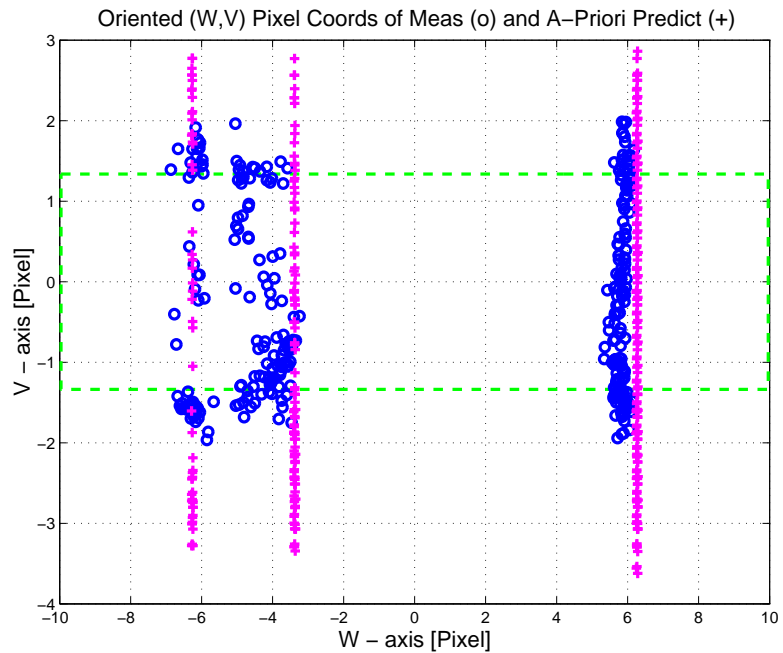


Figure 3.2: Oriented PixelCoords of measurements and a-priori predicts

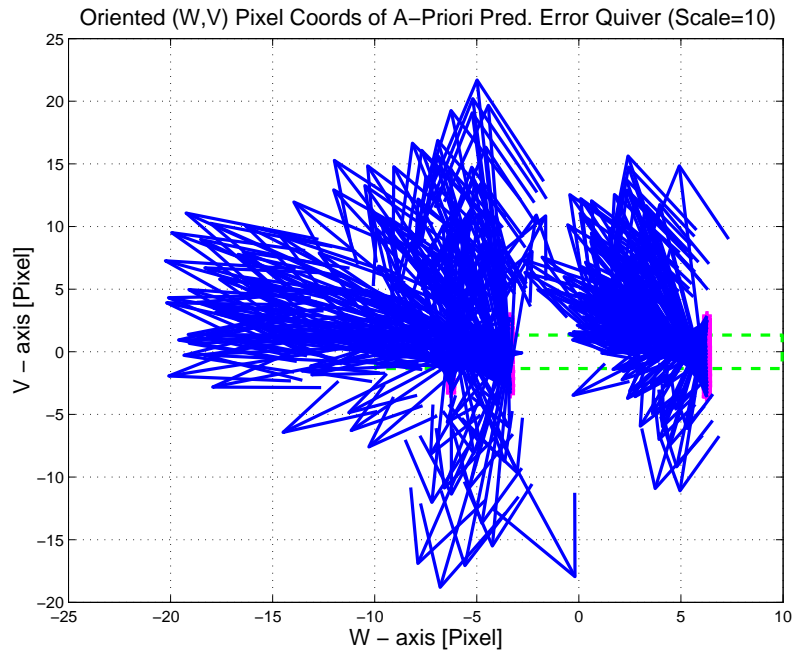


Figure 3.3: Oriented (W,V) Pixel Coords of A-Priori Prediction Error Quiver Plot

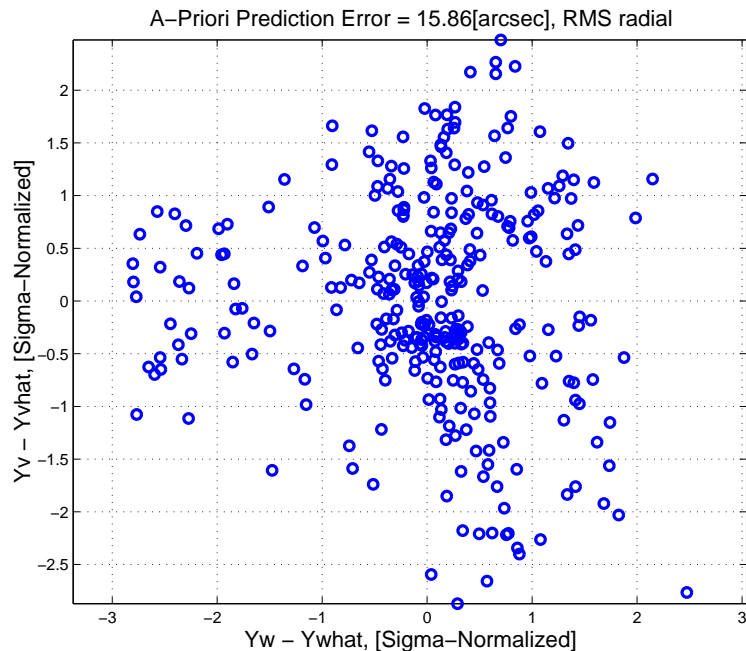


Figure 3.4: A-priori prediction error (Science Centroids)

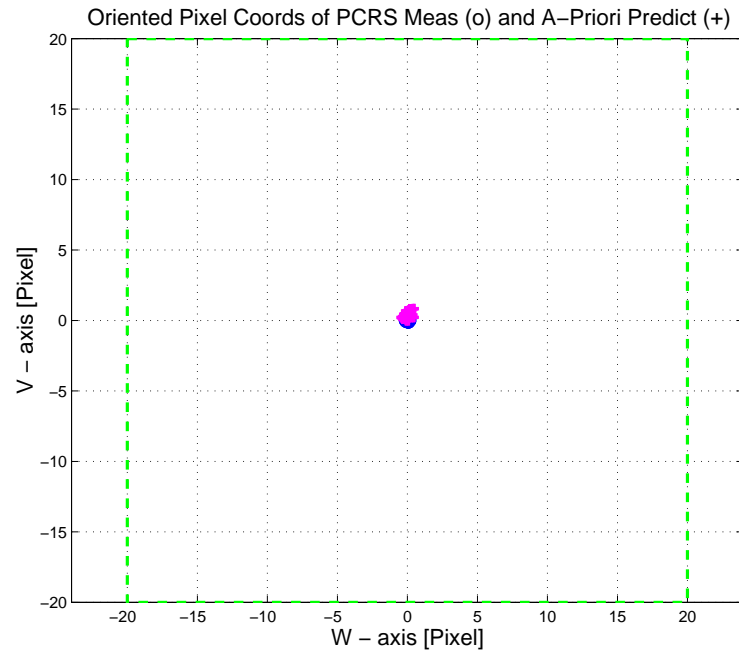


Figure 3.5: Oriented Pixel Coords of measurements and a-priori predicts (PCRS only)

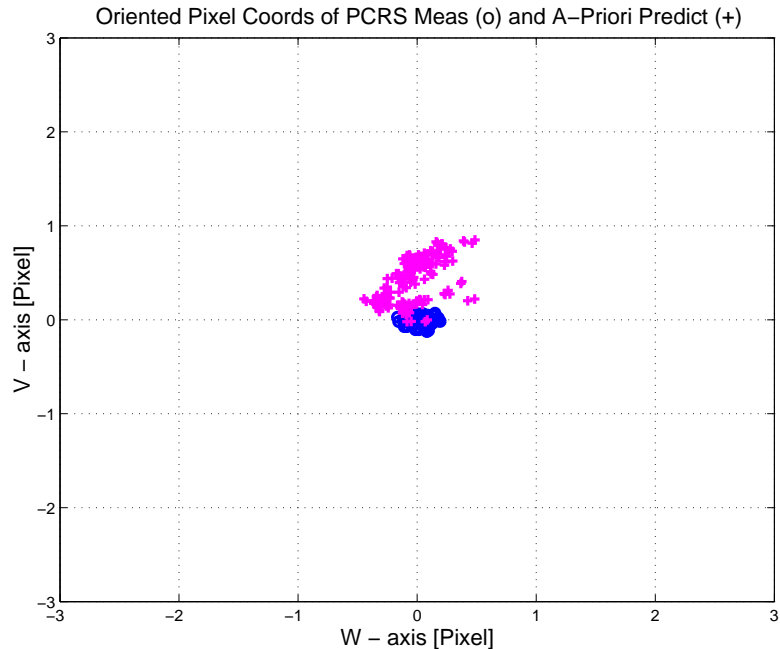


Figure 3.6: Oriented Pixel Coords of measurements and a-priori predicts (Zoomed, PCRS only)

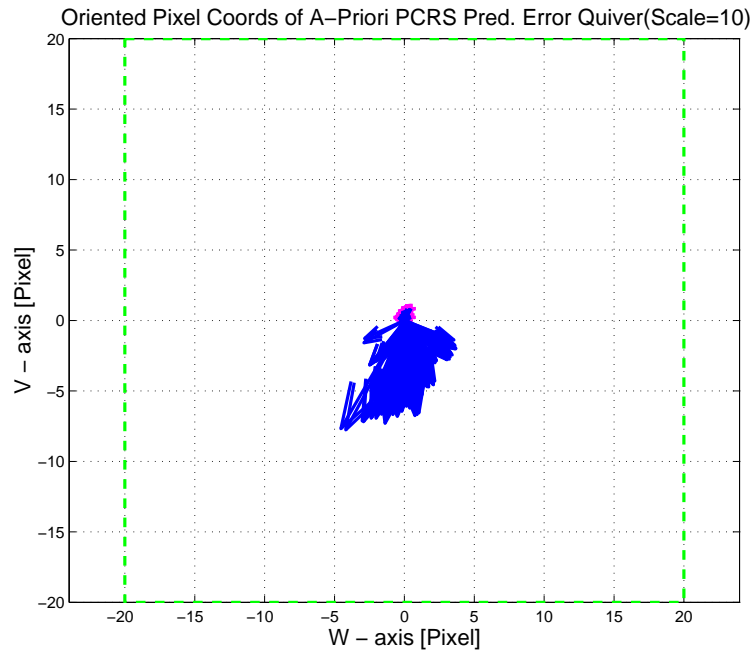


Figure 3.7: Oriented (W,V) PixelCoords of A-Priori PCRS Prediction Error Quiver Plot

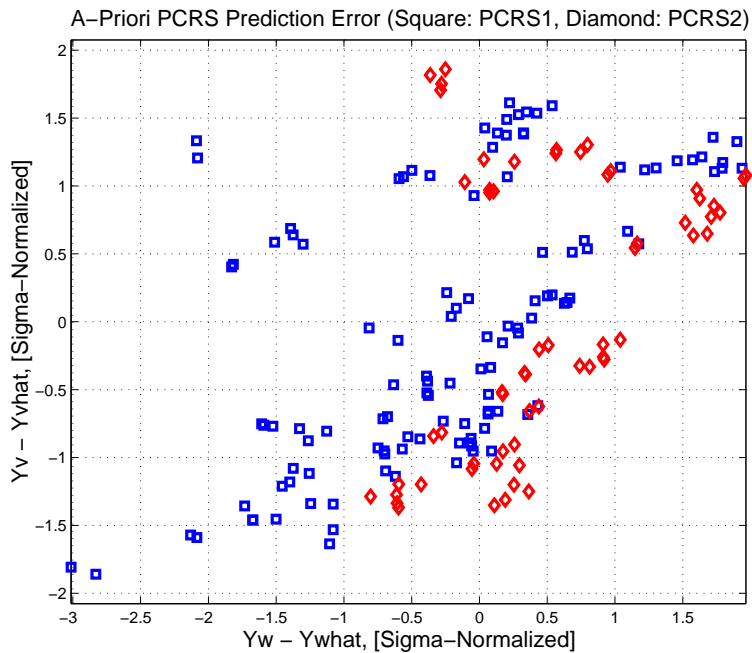


Figure 3.8: A-priori PCRS prediction error

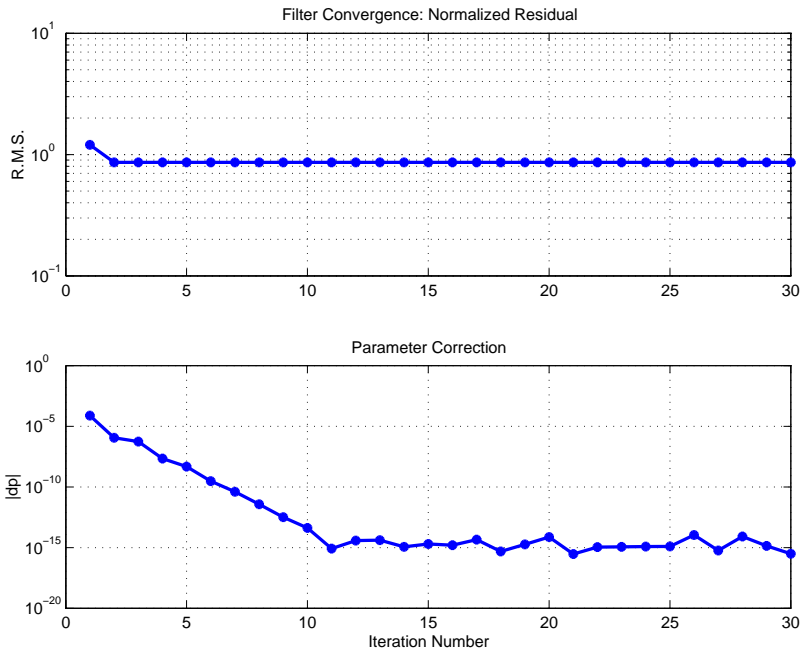


Figure 3.9: IPF execution convergence, chart 1

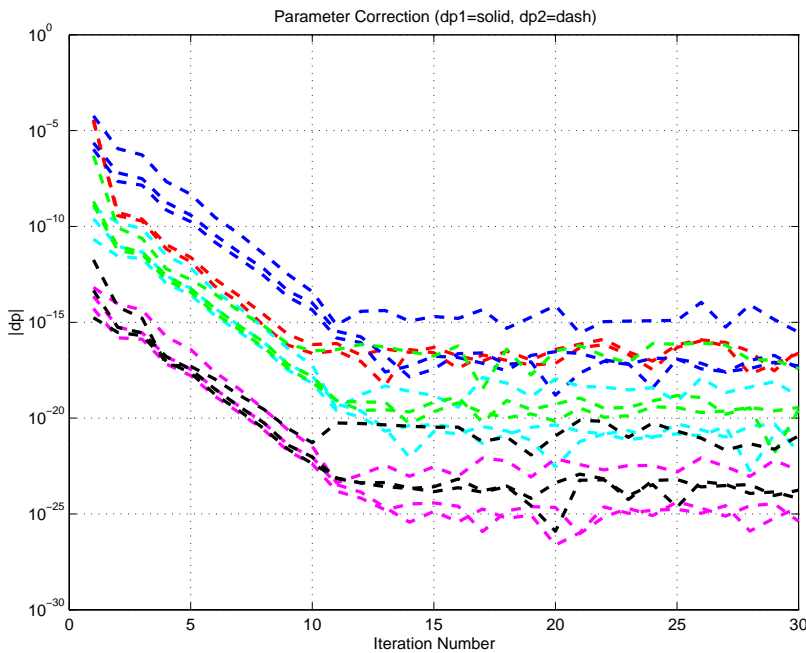


Figure 3.10: IPF execution convergence, chart 2

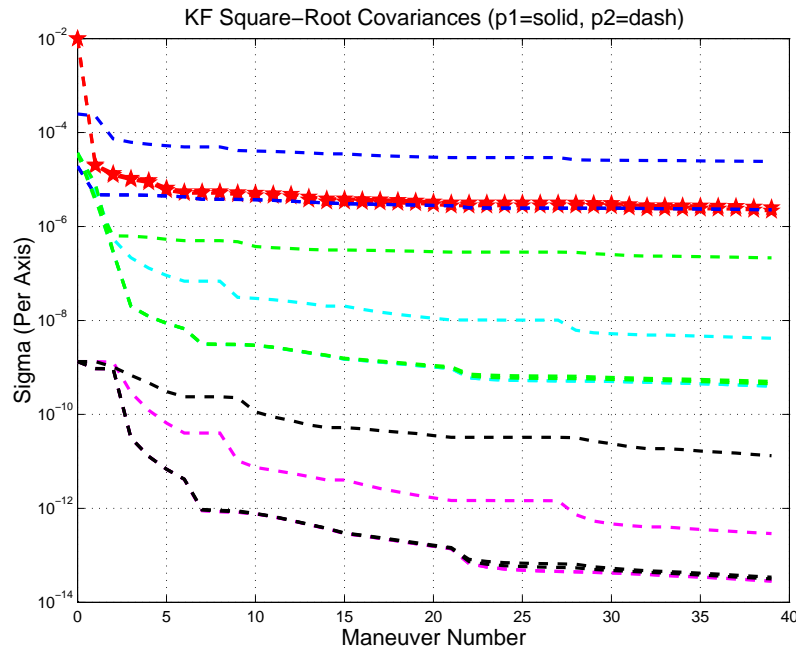


Figure 3.11: Parameter uncertainty convergence

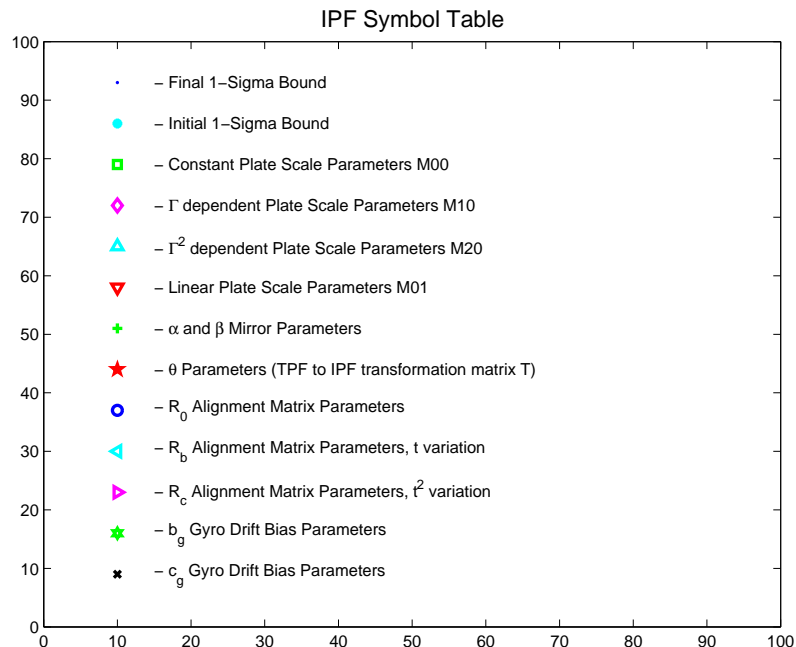


Figure 3.12: IPF parameter symbol table

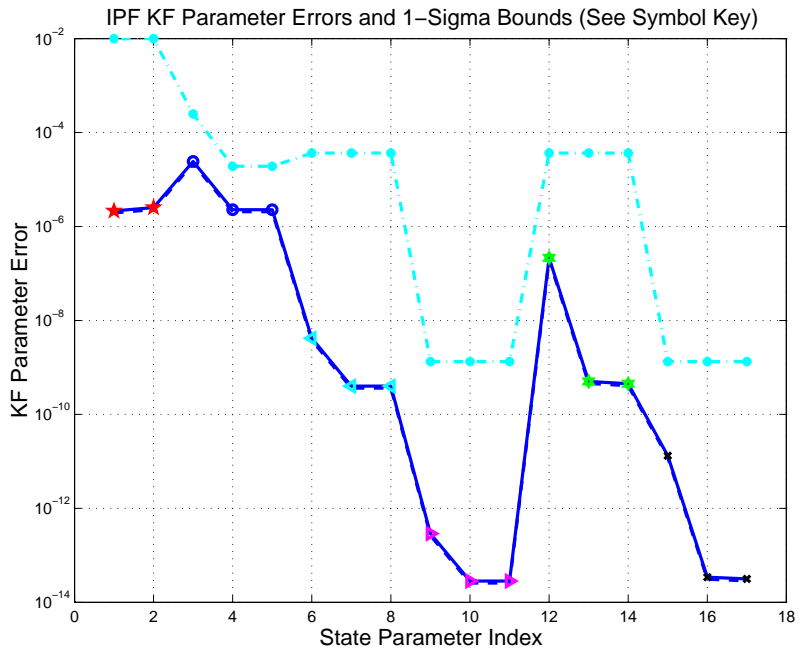


Figure 3.13: KF parameter error sigma plots

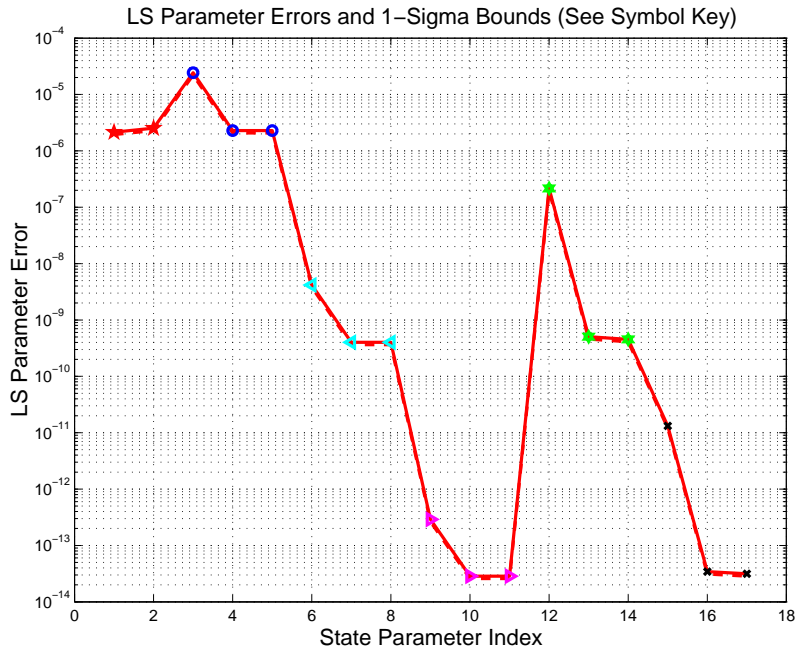


Figure 3.14: LS parameter error sigma plot

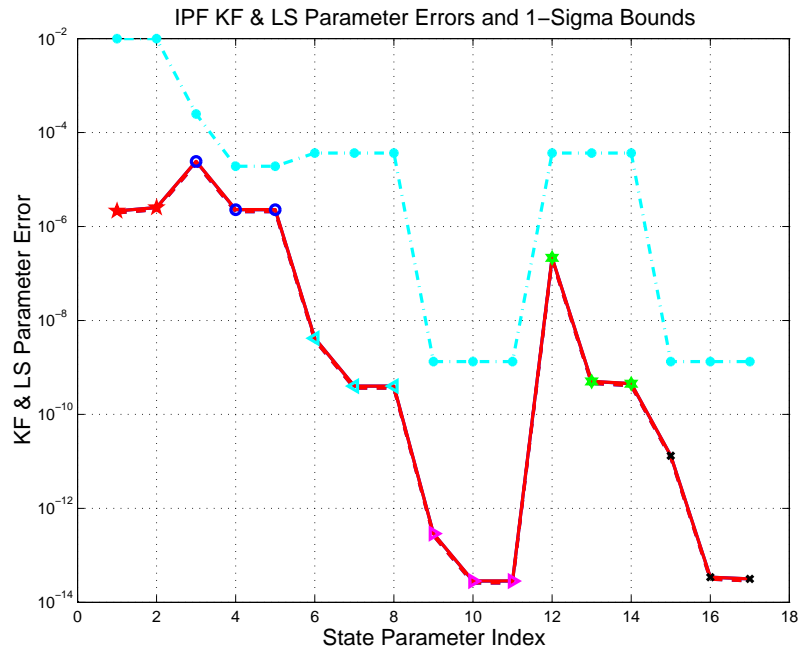


Figure 3.15: KF and LS parameter error sigma plot

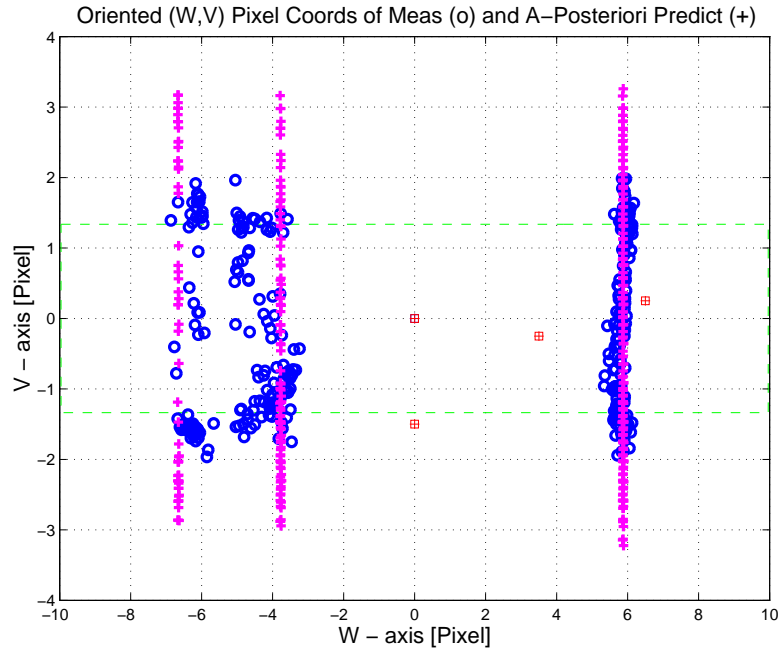


Figure 3.16: Oriented Pixel Coords of meas. and a-posteriori predicts

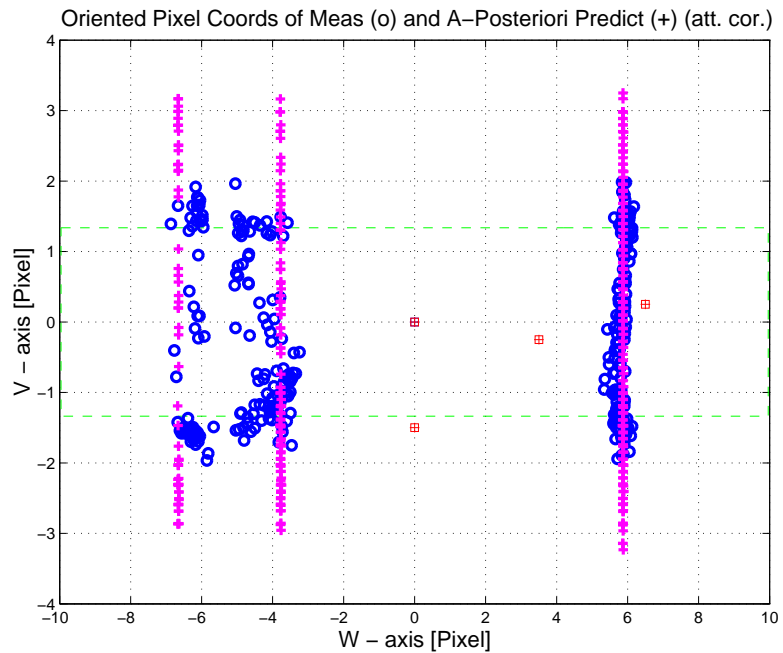


Figure 3.17: Oriented Pixel Coords of meas. and a-posteriori predicts (attitude corrected)

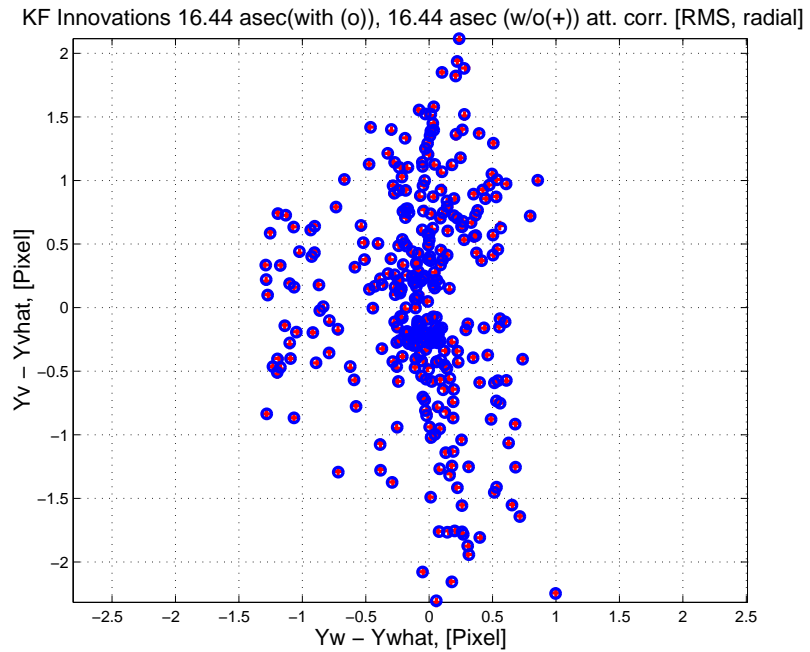


Figure 3.18: KF innovations with (o) and w/o (+) attitude corrections

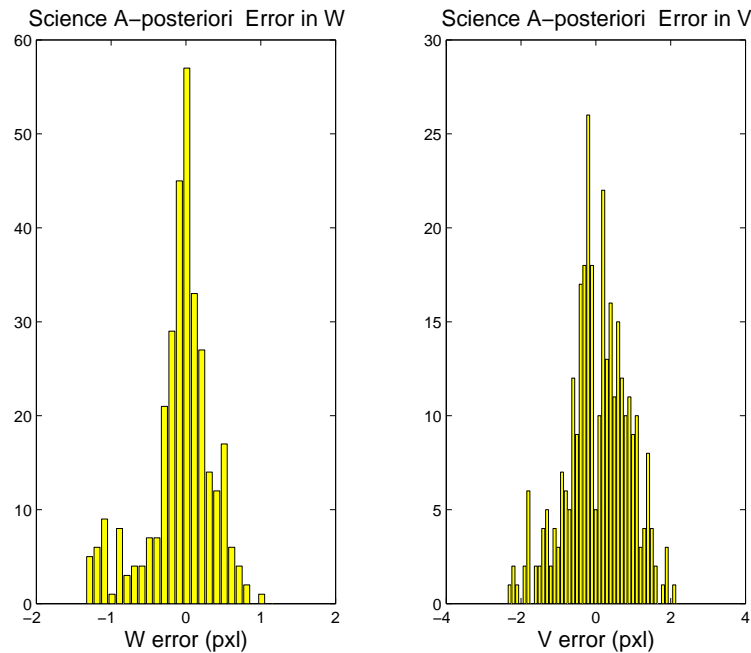


Figure 3.19: Histograms of science a-posteriori residuals (or innovations)

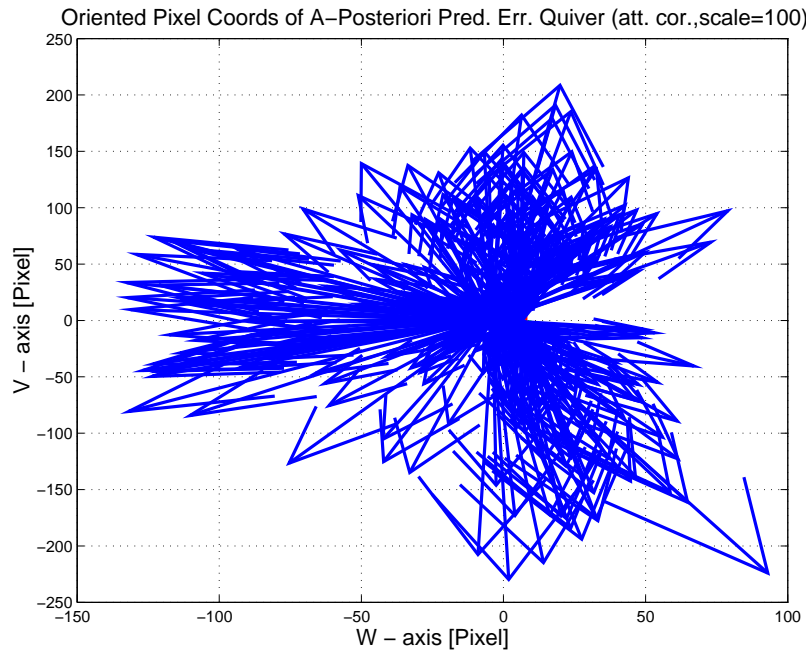


Figure 3.20: A-Posteriori Science Centroid Prediction Error Quiver (Att. Cor.)

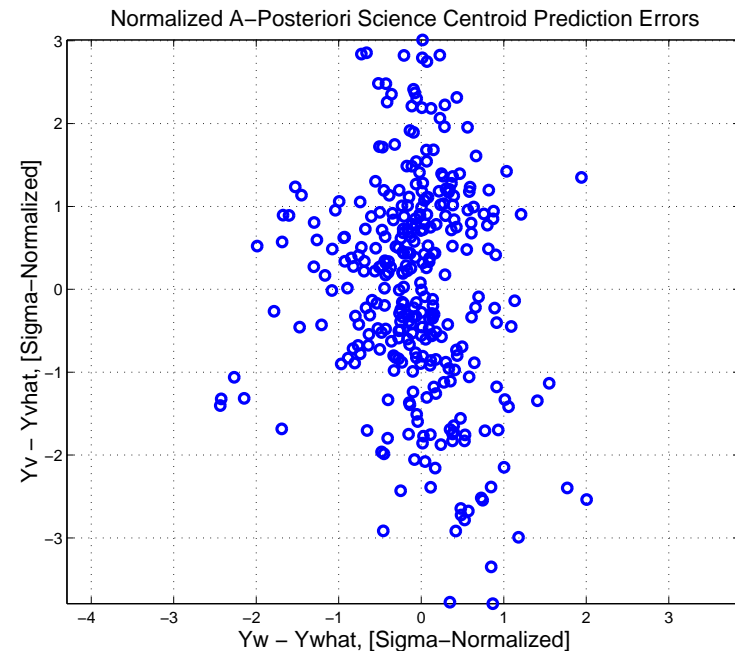


Figure 3.21: Normalized A-Posteriori Science Centroid Prediction Errors

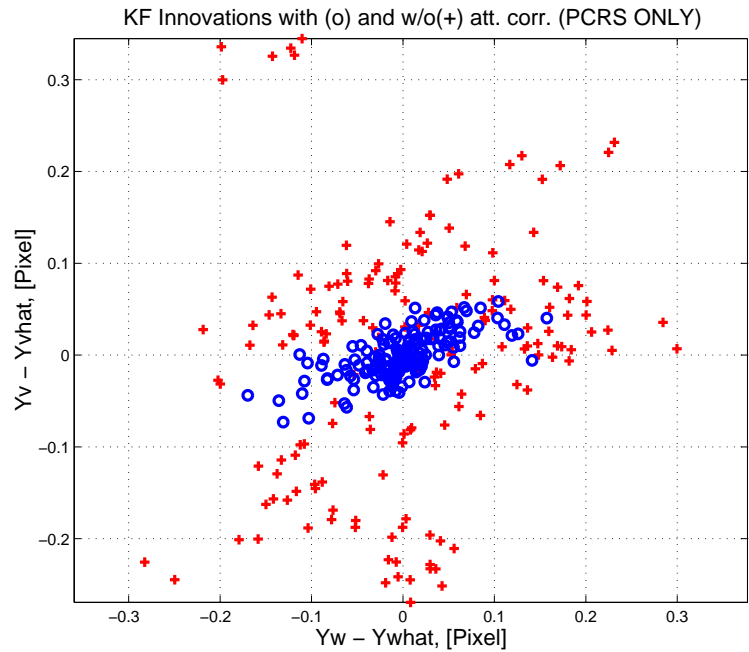


Figure 3.22: KF innovations with (o) and w/o (+) attitude corrections (PCRS)

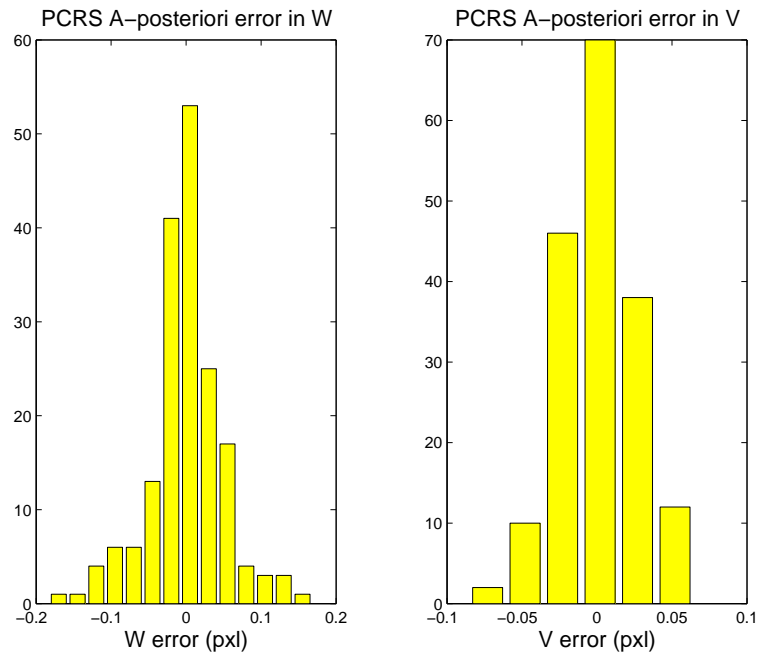


Figure 3.23: Histograms of PCRS a-posteriori residuals (or innovations)

IPF PCRS SUMMARY						
PCRS 1 (Total of 118 centroids)						
RMS	MEAN		SIGMA			
METRIC	APOST.	ATT. COR.	APOST.	ATT. COR.	STAT. CONF.	UNITS
Radial	0.0061	0.0036	0.1727	0.0640	0.0059	arcsec
W-axis	0.0058	-0.0000	0.1195	0.0582	0.0054	arcsec
V-axis	-0.0019	0.0036	0.1247	0.0266	0.0025	arcsec
PCRS 2 (Total of 60 centroids)						
METRIC	APOST.	ATT. COR.	APOST.	ATT. COR.	STAT. CONF.	UNITS
Radial	0.0091	0.0079	0.1664	0.0268	0.0035	arcsec
W-axis	-0.0010	0.0000	0.0993	0.0212	0.0027	arcsec
V-axis	0.0091	-0.0079	0.1335	0.0163	0.0021	arcsec
Combined (Total of 178 centroids)						
METRIC	APOST.	ATT. COR.	APOST.	ATT. COR.	STAT. CONF.	UNITS
Radial	0.0040	0.0003	0.1707	0.0546	0.0041	arcsec
W-axis	0.0035	-0.0000	0.1131	0.0489	0.0037	arcsec
V-axis	0.0018	-0.0003	0.1279	0.0243	0.0018	arcsec

Table 3.3: PCRS measurement prediction error summary

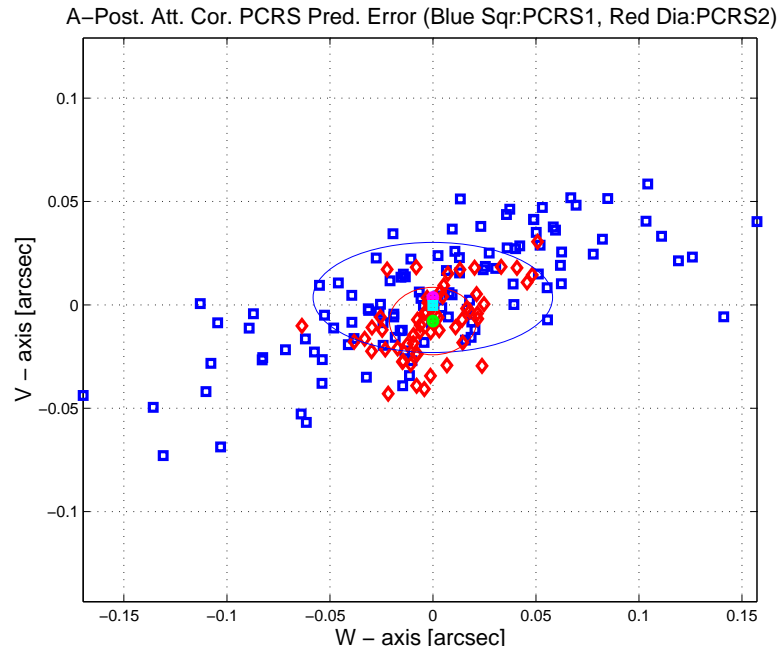


Figure 3.24: A-posteriori PCRS Prediction Summary

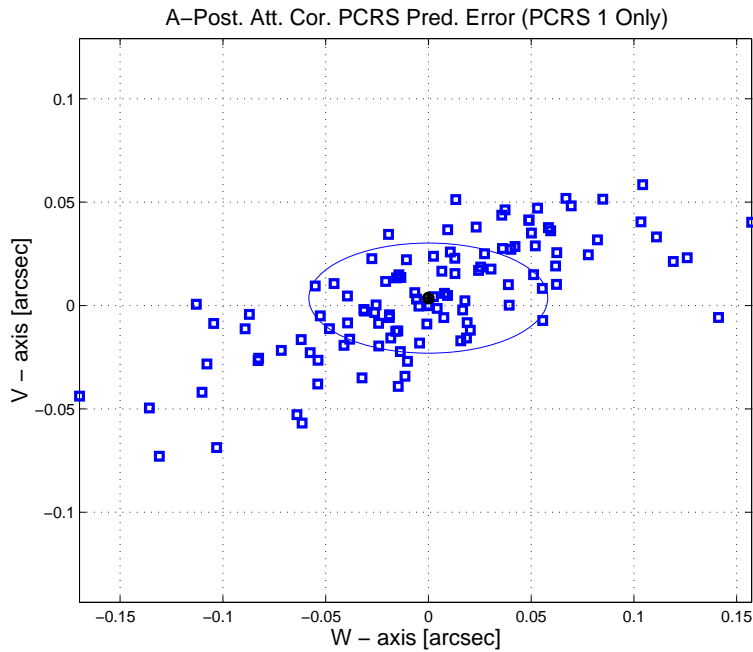


Figure 3.25: A-posteriori PCRS Prediction (PCRS 1 Only)

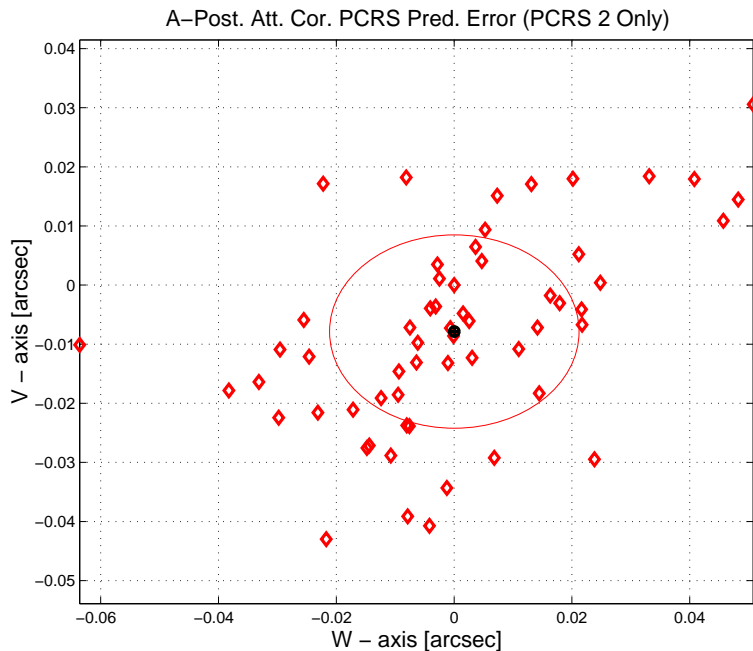


Figure 3.26: A-posteriori PCRS Prediction (PCRS 2 Only)

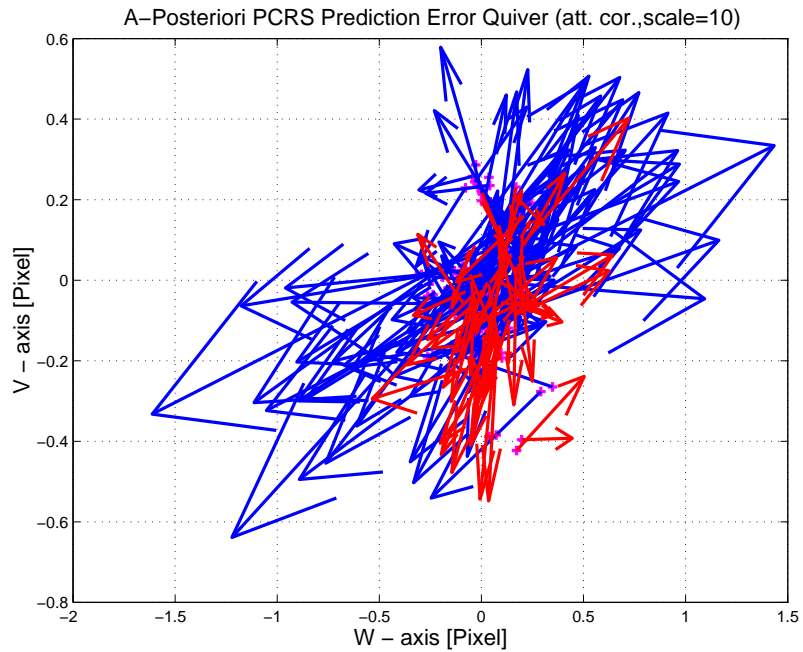


Figure 3.27: A–Posteriori PCRS Prediction Errors Quiver (Att. Cor.)

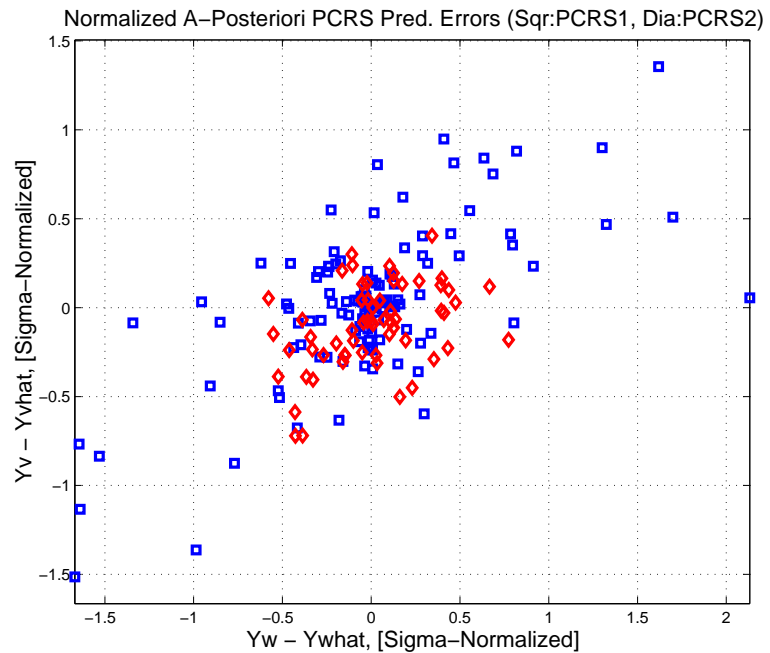


Figure 3.28: Normalized A–Posteriori PCRS Prediction Errors

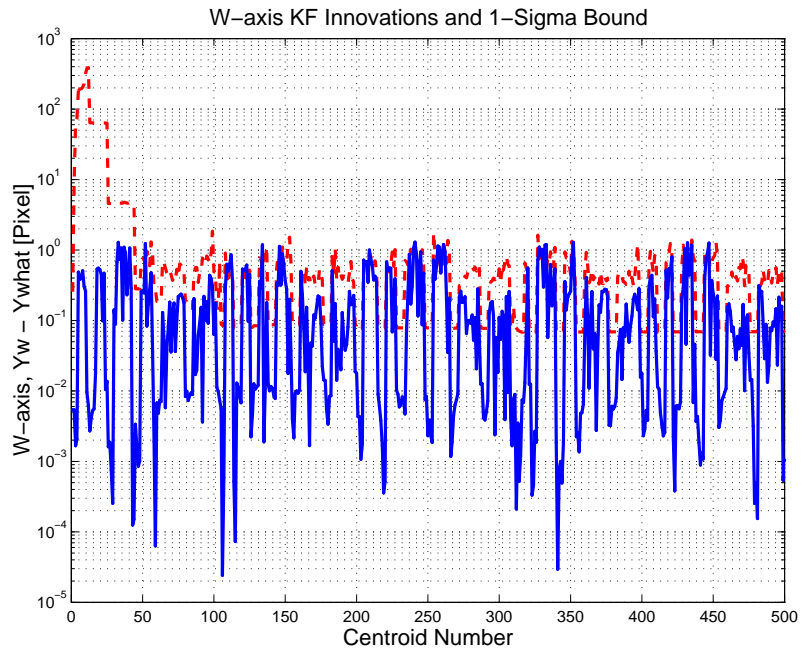


Figure 3.29: W-axis KF innovations and 1-sigma bound

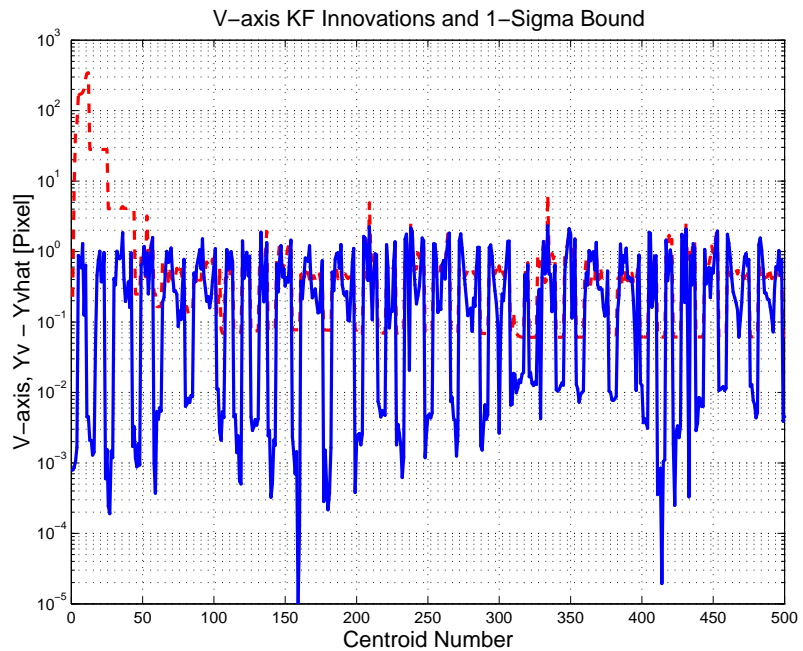


Figure 3.30: V-axis KF innovations and 1-sigma bound

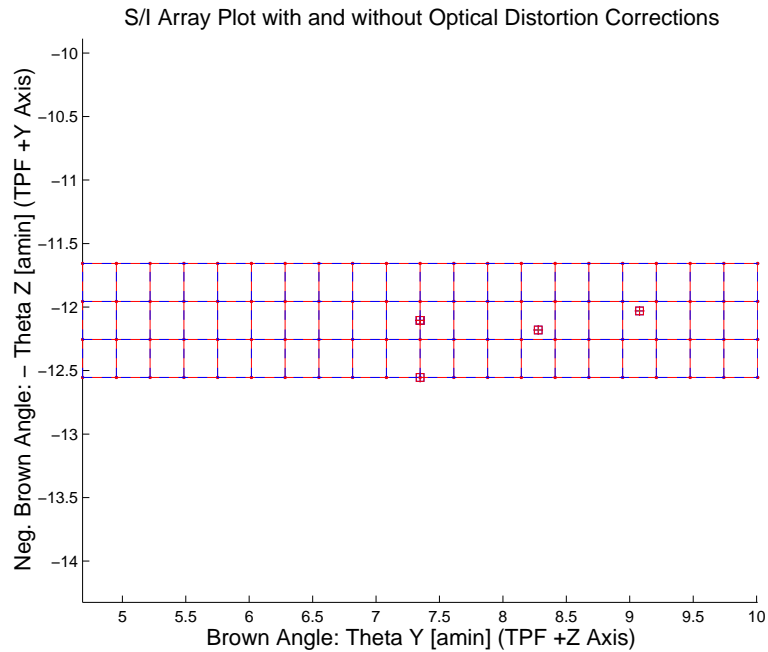


Figure 3.31: Array plot with (solid) and w/o (dashed) optical distortion corrections

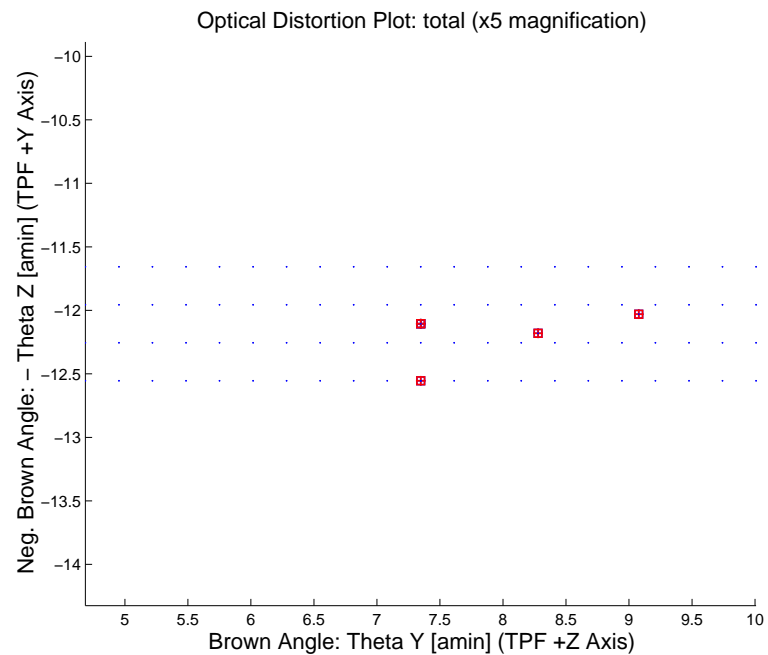


Figure 3.32: Optical Distortion Plot: total (x5 magnification)

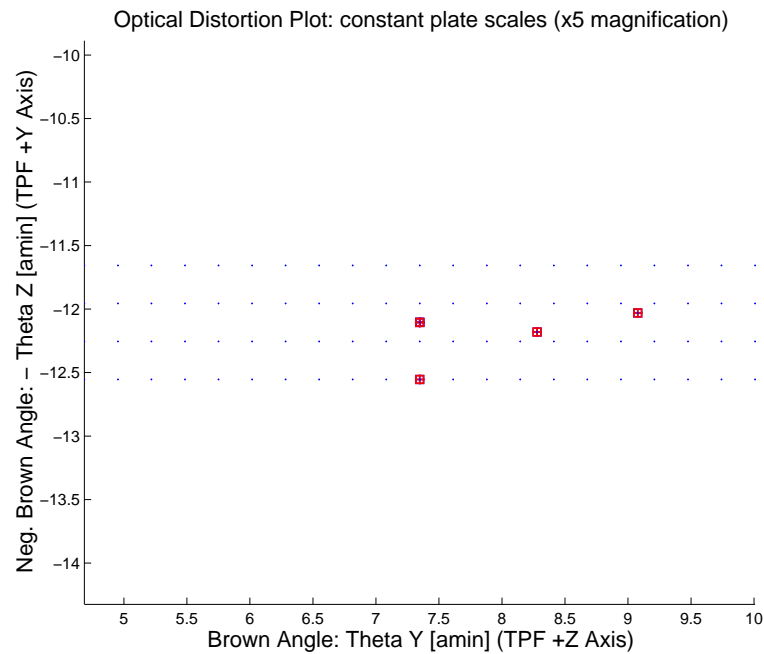


Figure 3.33: Optical Distortion Plot: constant plate scales (x5 magnification)

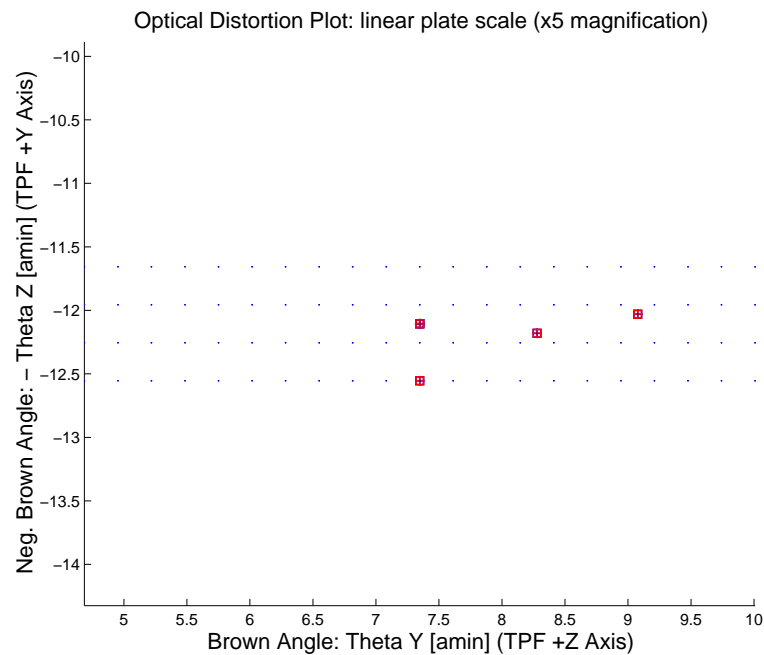


Figure 3.34: Optical Distortion Plot: linear plate scale (x5 magnification)

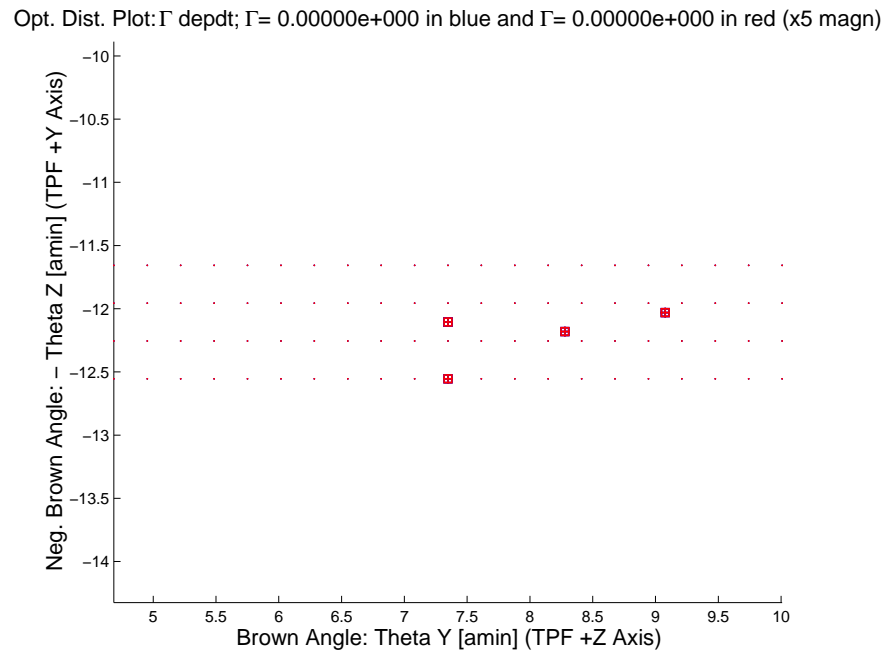


Figure 3.35: Optical Distortion Plot: gamma terms (x5 magnification)

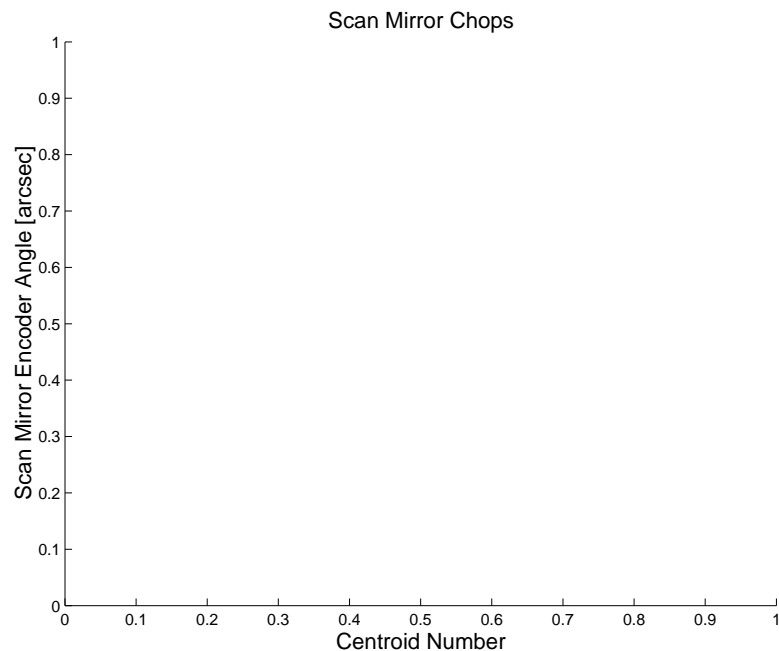


Figure 3.36: Scan Mirror Chops

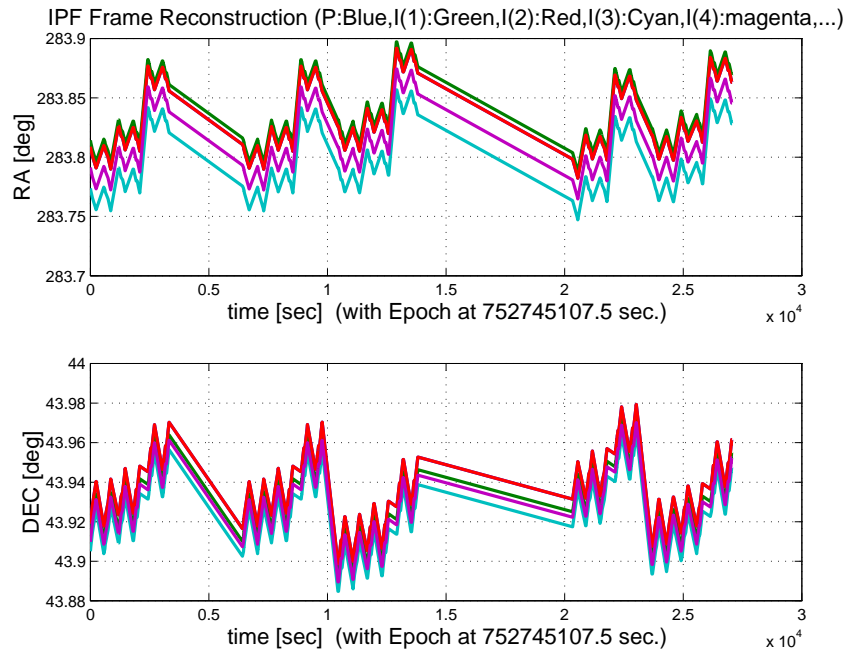


Figure 3.37: IPF Frame Reconstruction

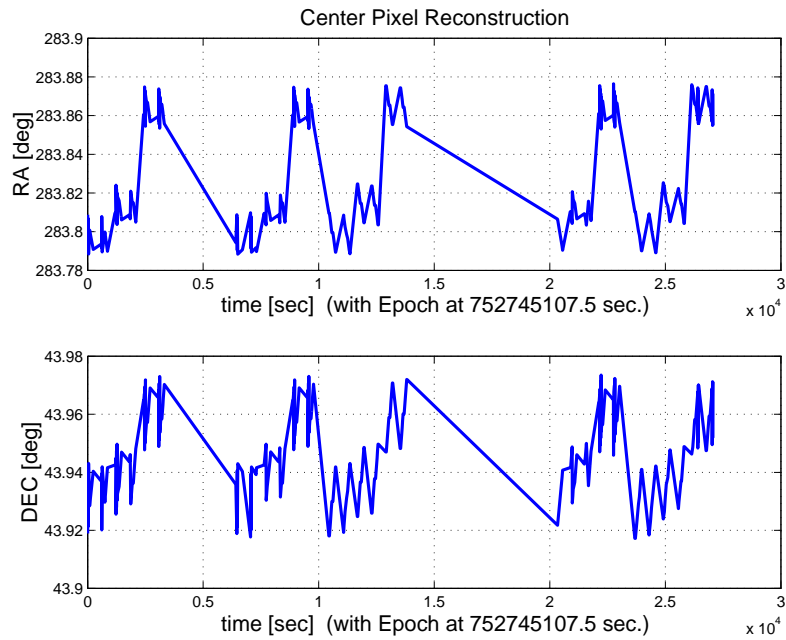


Figure 3.38: Center Pixel Reconstruction

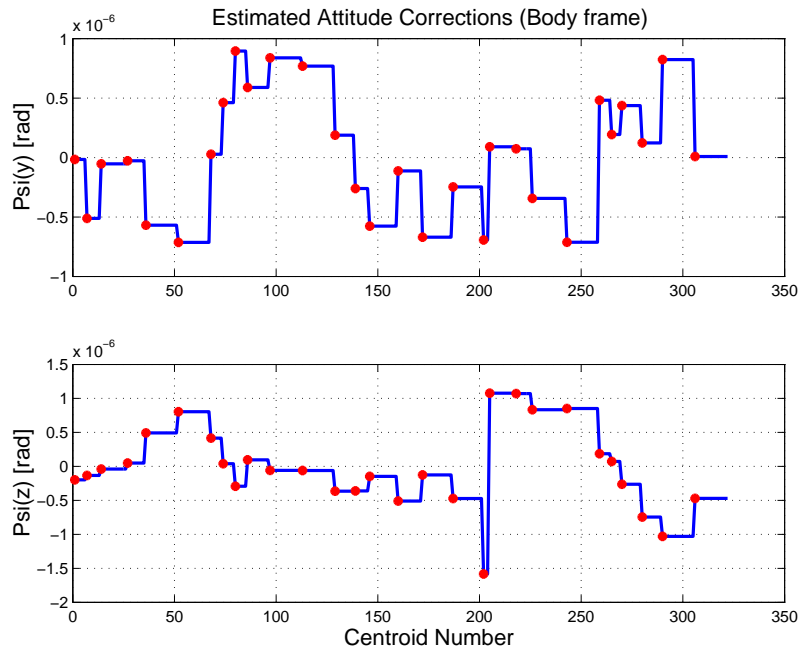


Figure 3.39: Estimated attitude corrections (Body frame)

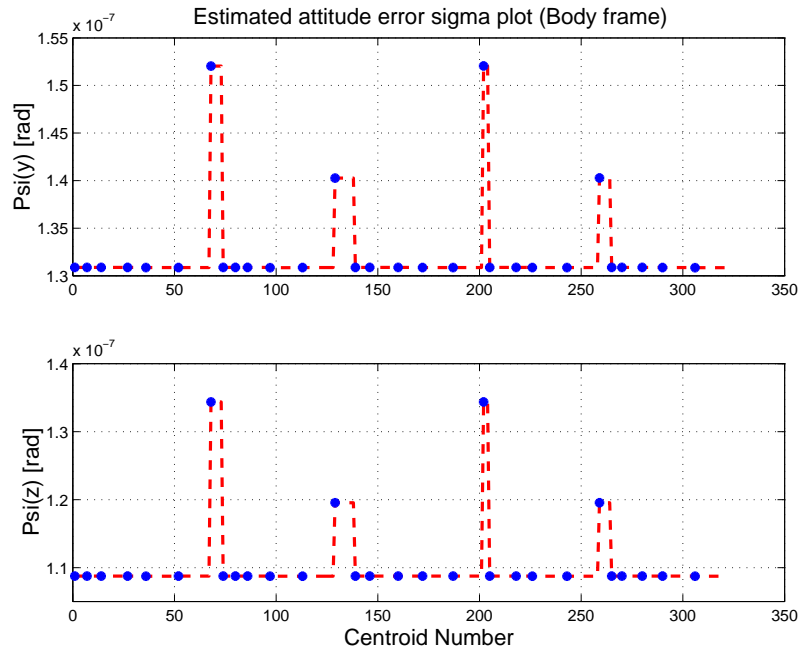


Figure 3.40: Estimated attitude error sigma plot (Body frame)

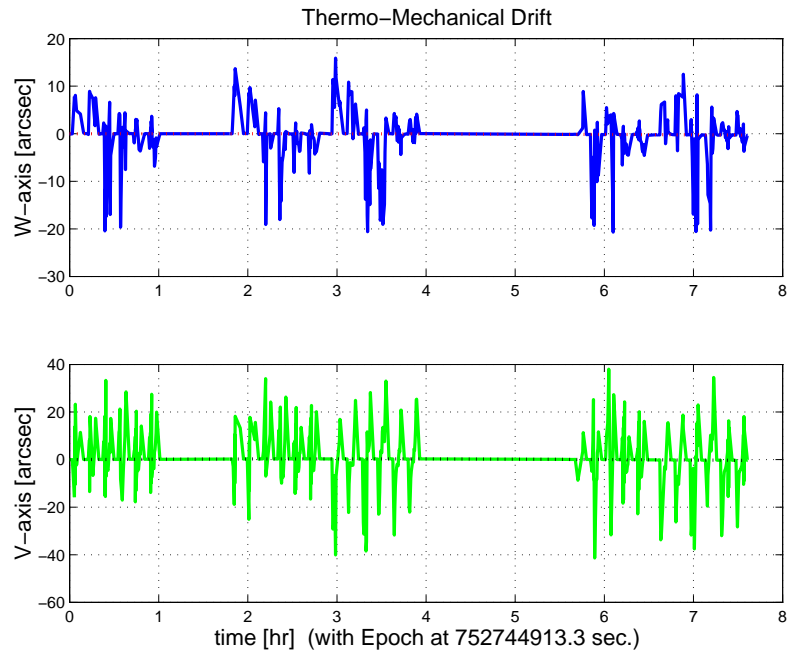


Figure 3.41: Thermo-mechanical boresight drift (equiv. angle in (W,V) coords)

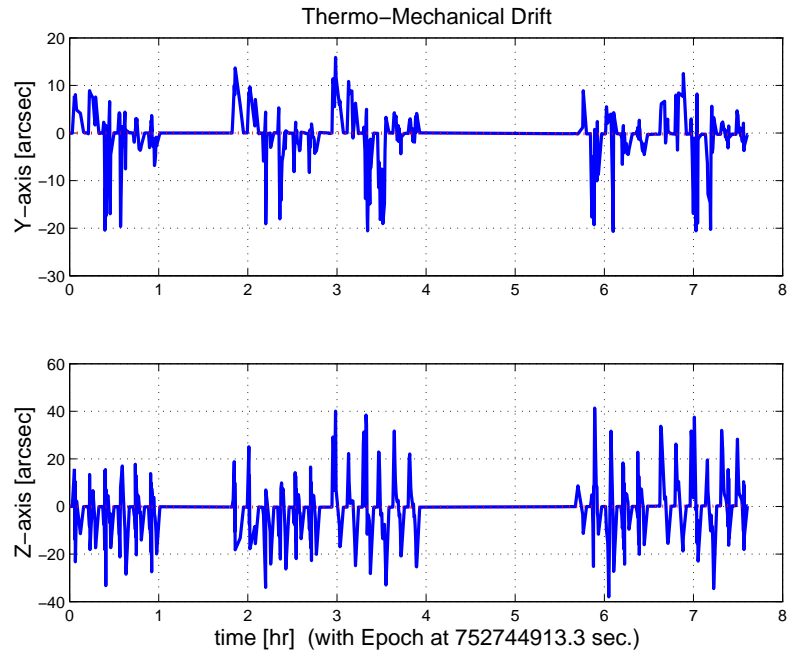


Figure 3.42: Thermo-mechanical boresight drift (equiv. angle in Body frame)

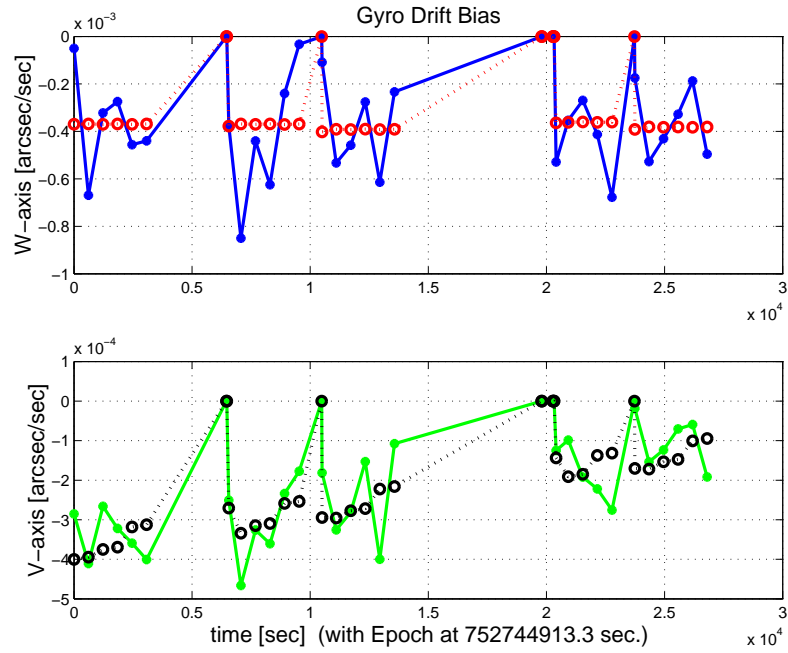


Figure 3.43: Gyro drift bias contribution (equiv. rate in (W,V) coords)

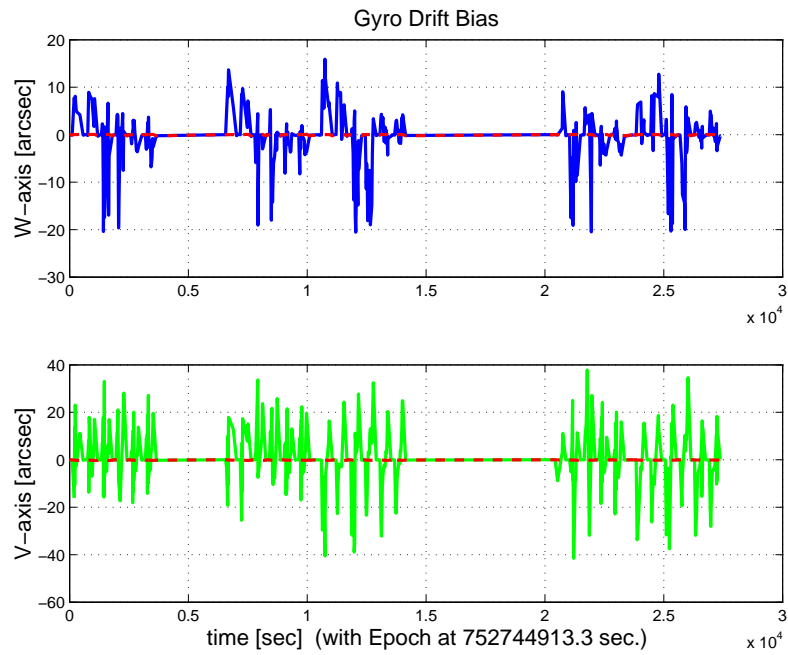


Figure 3.44: Gyro drift bias contribution (equiv. angle in (W,V) coords)

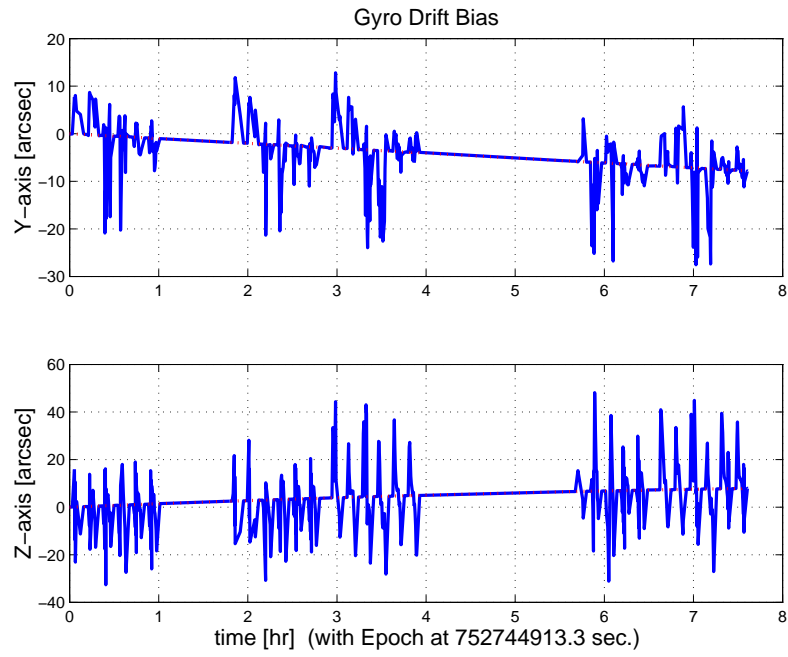


Figure 3.45: Gyro drift bias contribution (equiv. angle in Body frame)

## 3.2 IPF OUTPUT DATA (IF MINI FILE)

```

OUTPUT FILE NAME: IFmini502087.dat    DATE: 20-Nov-2003    TIME: 19:00
INSTRUMENT NAME: MIPS_160um_center_large_FOV   NF: 87
IPF FILTER VERSION: IPF.V3.0.0B      SW RELEASE DATE: November 3, 2003
FRAME TABLE USED: BodyFrames_FTU_13Aa
-----
----- IPF BROWN ANGLE SUMMARY -----
----- WAS -----      ----- IS -----
Frame  theta_Y     theta_Z     angle      theta_Y     theta_Z     angle
Number (arcmin) (arcmin) (deg)      (arcmin) (arcmin) (deg)
----- -----
087    +7.240265 +11.975320 +0.000002 +7.347515 +12.105588 +0.000006
088    +7.240265 +12.424391 +0.000002 +7.347515 +12.554659 +0.000006
089    +7.240265 +11.975320 +0.000002 +7.347515 +12.105588 +0.000006
091    +8.969800 +12.050100 +0.000000 +9.077043 +12.030743 +0.000006
092    +8.171600 +11.900500 -0.000000 +8.278799 +12.180433 +0.000006
-----
OFFSET      NF      Delta_CW      Delta_CV
  0        87      +0.000      +0.000      pixels
OFFSET FRAME NAME: MIPS_160um_center_large_FOV
Brown Angle  theta_Y(arcmin)  theta_Z(arcmin)  angle(deg)
WAS(FTB)      +7.240265      +11.975320      +0.000002
IS (EST)      +7.347515      +12.105588      +0.000006
dT_EST       +0.107249      +0.130267      +0.000005
T_ssSIGMA    +0.006693      +0.007863      +999.999999
dT_EST/T_ssSIGMA +16.023499      +16.567820      +999.999999
-----
OFFSET      NF      Delta_CW      Delta_CV
  1        88      +0.000      -1.500      pixels
OFFSET FRAME NAME: MIPS_160um_plusY_edge
Brown Angle  theta_Y(arcmin)  theta_Z(arcmin)  angle(deg)
WAS(FTB)      +7.240265      +12.424391      +0.000002
IS (EST)      +7.347515      +12.554659      +0.000006
dT_EST       +0.107249      +0.130267      +0.000005
T_ssSIGMA    +0.006693      +0.007863      +999.999999
dT_EST/T_ssSIGMA +16.023493      +16.567824      +999.999999
-----
OFFSET      NF      Delta_CW      Delta_CV
  2        89      +0.000      +0.000      pixels
OFFSET FRAME NAME: MIPS_160um_large_only
Brown Angle  theta_Y(arcmin)  theta_Z(arcmin)  angle(deg)
WAS(FTB)      +7.240265      +11.975320      +0.000002
IS (EST)      +7.347515      +12.105588      +0.000006
dT_EST       +0.107249      +0.130267      +0.000005
T_ssSIGMA    +0.006693      +0.007863      +999.999999
dT_EST/T_ssSIGMA +16.023499      +16.567820      +999.999999
-----
OFFSET      NF      Delta_CW      Delta_CV
  3        91      +6.500      +0.250      pixels
OFFSET FRAME NAME: MIPS_160um_small_FOV1
Brown Angle  theta_Y(arcmin)  theta_Z(arcmin)  angle(deg)
WAS(FTB)      +8.969800      +12.050100      +0.000000
IS (EST)      +9.077043      +12.030743      +0.000006
dT_EST       +0.107243      -0.019357      +0.000006
T_ssSIGMA    +0.006693      +0.007863      +999.999999
dT_EST/T_ssSIGMA +16.022492      -2.461941      +999.999999
-----
OFFSET      NF      Delta_CW      Delta_CV
  4        92      +3.500      -0.250      pixels
OFFSET FRAME NAME: MIPS_160um_small_FOV2

```

Brown Angle	theta_Y(arcmin)	theta_Z(arcmin)	angle(deg)
WAS(FTB)	+8.171600	+11.900500	-0.000000
IS (EST)	+8.278799	+12.180433	+0.000006
dT_EST	+0.107199	+0.279933	+0.000006
T_ssSIGMA	+0.006693	+0.007863	+999.999999
dT_EST/T_ssSIGMA	+16.015972	+35.602766	+999.999999

---

VARNAME	MEAN	SIGMA	SCALED_SIGMA
del_theta2	-3.6766153289842550E-017	+2.1464360729121769E-006	+1.9469899121277889E-006
del_theta3	-2.4494922285173484E-017	+2.5214521003412253E-006	+2.2871595689393991E-006
del_arx	+3.0265297180651963E-016	+2.4258745993793997E-005	+2.2004630991271940E-005
del_ary	+3.8697581142665080E-018	+2.2701184770533382E-006	+2.0591797864080122E-006
del_arz	+5.3126899068524781E-018	+2.2704229981242484E-006	+2.0594560114773608E-006
brx	+1.0606092197625871E-009	+4.1736952915969240E-009	+3.7858768456166123E-009
bry	+2.0742084965886971E-011	+3.98977977950548553E-010	+3.6190670462699293E-010
brz	-2.5461544645109712E-010	+3.989875200434471E-010	+3.6191575048441332E-010
crx	-7.0780503591000624E-014	+2.9038090199214807E-013	+2.6339880045261096E-013
cry	-5.1808235406633813E-015	+2.8363629796687038E-014	+2.5728090289943776E-014
crz	+2.3119465669793647E-014	+2.8363589388062912E-014	+2.5728053636076220E-014
bgx	+4.9468799417466938E-007	+2.1496862982075243E-007	+1.9499381275170308E-007
bgy	-1.3578901509034456E-009	+5.0415182346340678E-010	+4.5730619553571251E-010
bgz	+2.0301659685871481E-009	+4.5117937774564018E-010	+4.0925593271409602E-010
cgx	-1.8032082874848952E-012	+1.3238290513384259E-011	+1.2008192747341493E-011
cgy	-1.8147169213134564E-015	+3.4208598151895546E-014	+3.1029946034875034E-014
cgz	-4.6064414451173017E-014	+3.1408978189833138E-014	+2.8490465873916095E-014

---

LSQF RESIDUAL SIGMA SCALE =	+9.0708031638986131E-001
-----------------------------	--------------------------

---

qT	qT(1)	qT(2)	qT(3)	qT(4)
FrmTbl:	-1.8193149813468900E-006	-1.0530521324111301E-003	-1.7417378662919600E-003	+9.9999792871140503E-001
Estim:	-1.8265322546296884E-006	-1.0686509308528733E-003	-1.7606843785389161E-003	+9.9999787898393622E-001
DelTheta	deltheta(1)	deltheta(2)	deltheta(3)	
	+5.9109568302960632E-010	-3.1197593193008466E-005	-3.7893160804976991E-005	[rad]
EulAngT	theta(1)	theta(2)	theta(3)	
Mean	+1.1005749045188268E-007	-2.1373053875757175E-003	-3.5213727048114224E-003	
SigmaT	+9.9999000000000000E+004	+2.1464360729121769E-006	+2.5214521003412253E-006	

---

qR	qR(1)	qR(2)	qR(3)	qR(4)
ASFFILE:	+7.1086635580286384E-004	+1.2695571640506387E-003	-1.6159859660547227E-004	+9.9999892711639404E-001
Estim:	+6.8112714676337664E-004	+1.2700874373012666E-003	-1.6039476083620020E-004	+9.9999894860806349E-001
DelThetaR	delthetaR(1)	delthetaR(2)	delthetaR(3)	
	-5.9481611737891024E-005	+1.0526600363196096E-006	+2.3313794398765295E-006	[rad]
EulAngR	angR(1)	angR(2)	angR(3)	
Mean	+1.3618502458919803E-003	+2.5403934347805511E-003	-3.1906003728778069E-004	
SigmaR	+2.4258745993793997E-005	+2.2701184770533382E-006	+2.2704229981242484E-006	

---

Initial Gyro Bias	Bg0(1)	Bg0(2)	Bg0(3)
	-4.1339711742693908E-007	-2.0063052375007828E-007	+3.6787506019209104E-007
Gyro Bias Correction	Bg(1)	Bg(2)	Bg(3)
	+4.9468799417466938E-007	-1.3578901509034456E-009	+2.0301659685871481E-009
Total Gyro Bias	BgT(1)	BgT(2)	BgT(3)
	+8.1290876747730308E-008	-2.0198841390098173E-007	+3.6990522616067818E-007

---

Initial Gyro Bias Rate	Cg0(1)	Cg0(2)	Cg0(3)
	+0.0000000000000000E+000	+0.0000000000000000E+000	+0.0000000000000000E+000
Gyro Bias Rate Correction	Cg(1)	Cg(2)	Cg(3)
	-1.8032082874848952E-012	-1.8147169213134564E-015	-4.6064414451173017E-014
Total Gyro Bias Rate	CgT(1)	CgT(2)	CgT(3)
	-1.8032082874848952E-012	-1.8147169213134564E-015	-4.6064414451173017E-014

---

---

OFFSET	NF	Delta_CW	Delta_CV	
1	88	+0.000	-1.500	pixels
OFFSET FRAME NAME: MIPS_160um_plusY_edge				
qT	qT(1)	qT(2)	qT(3)	qT(4)
WAS(FTB)	-1.8880947946946114E-006	-1.0530520004150409E-003	-1.8070524774803814E-003	+9.9999781281723976E-001
IS (EST)	-1.8963308941670108E-006	-1.0686507929678472E-003	-1.8259989907623182E-003	+9.9999776185228151E-001
DelTheta	deltheta(1)	deltheta(2)	deltheta(3)	
Units	rad	rad	rad	
EulAngT	theta(1)	theta(2)	theta(3)	[rad]
Mean	+1.1005749045188268E-007	-2.1373053549634869E-003	-3.6520022139294368E-003	
sSigmaT	+2.5433375484681475E-010	+1.94698998923010515E-006	+2.2871595716762562E-006	
SigmaT	+2.8038724934419436E-010	+2.1464360510544243E-006	+2.5214521033584414E-006	

---

OFFSET	NF	Delta_CW	Delta_CV	
2	89	+0.000	+0.000	pixels
OFFSET FRAME NAME: MIPS_160um_large_only				
qT	qT(1)	qT(2)	qT(3)	qT(4)
WAS(FTB)	-1.8193149813468912E-006	-1.0530521324111307E-003	-1.7417378662919611E-003	+9.9999792871140569E-001
IS (EST)	-1.8265322546296893E-006	-1.0686509308528737E-003	-1.7606843785389163E-003	+9.9999787898393622E-001
DelTheta	deltheta(1)	deltheta(2)	deltheta(3)	
Units	rad	rad	rad	
EulAngT	theta(1)	theta(2)	theta(3)	[rad]
Mean	+1.1005749045188266E-007	-2.1373053875757175E-003	-3.5213727048114232E-003	
sSigmaT	+1.6901983101471378E-024	+1.9469899121277893E-006	+2.2871595689394000E-006	
SigmaT	+1.8633391989741889E-024	+2.1464360729121773E-006	+2.5214521003412262E-006	

---

OFFSET	NF	Delta_CW	Delta_CV	
3	91	+6.500	+0.250	pixels
OFFSET FRAME NAME: MIPS_160um_small_FOV1				
qT	qT(1)	qT(2)	qT(3)	qT(4)
WAS(FTB)	-2.2864689507497608E-006	-1.3046021533220905E-003	-1.7526136129115506E-003	+9.9999761317391034E-001
IS (EST)	-2.2550603563025661E-006	-1.3202000341957770E-003	-1.7497980854334571E-003	+9.9999759763383667E-001
DelTheta	deltheta(1)	deltheta(2)	deltheta(3)	
Units	rad	rad	rad	
EulAngT	theta(1)	theta(2)	theta(3)	[rad]
Mean	+1.1005749045188268E-007	-2.6404046850177529E-003	-3.4996011517975170E-003	
sSigmaT	+1.1516620852389911E-009	+1.9469899122021944E-006	+2.2871592789256653E-006	
SigmaT	+1.2696362873604778E-009	+2.1464360729942044E-006	+2.5214517806190040E-006	

---

OFFSET	NF	Delta_CW	Delta_CV	
4	92	+3.500	-0.250	pixels
OFFSET FRAME NAME: MIPS_160um_small_FOV2				
qT	qT(1)	qT(2)	qT(3)	qT(4)
WAS(FTB)	-2.0571418166958298E-006	-1.1885089828493499E-003	-1.7308554769085395E-003	+9.9999779578831283E-001
IS (EST)	-2.0781242430031006E-006	-1.2041004277977840E-003	-1.7715698889046484E-003	+9.9999770583635350E-001
DelTheta	deltheta(1)	deltheta(2)	deltheta(3)	
Units	rad	rad	rad	
EulAngT	theta(1)	theta(2)	theta(3)	[rad]
Mean	+1.1005749045188268E-007	-2.4082050215840454E-003	-3.5431443322051148E-003	
sSigmaT	+6.2082604519870210E-010	+1.9469899111305084E-006	+2.2871594855299159E-006	
SigmaT	+6.8442235376638062E-010	+2.1464360718127370E-006	+2.5214520083874243E-006	

---

```

-----  

          q(1)           q(2)           q(3)           q(4)  

PCRS1A: +5.3371888965461637E-007 +3.7444233778550031E-004 -1.4253684912431913E-003 +9.9999891405806784E-001  

PCRS2A: -5.2779261998836216E-007 +3.8462959425181312E-004 +1.3722087221825403E-003 +9.9999898455099423E-001  

-----  

***** CS-FILE PARAMETERS: ***** AS-FILE PARAMETERS: *****  

Row (01) PIX2RADX: +7.7399898172000000E-005 Row (1) TASTART: +7.5274400029071045E+008  

Row (02) PIX2RADY: +8.708614099900005E-005 Row (2) TASTOP: +7.5277300039073789E+008  

Row (03) CX0: +1.0500000000000000E+001 Row (3) S/C TIME: +7.5271691689080811E+008  

Row (04) CY0: +2.0000000000000000E+000 Row (4) QR1: +7.1086635580286384E-004  

Row (05) BETA0: +2.8047410000000001E-006 Row (5) QR2: +1.2695571640506387E-003  

Row (06) GAMMA_E0: +2.0070000000000000E+003 Row (6) QR3: -1.6159859660547227E-004  

Row (07) D11: -1.0000000000000000E+000 Row (7) QR4: +9.9999892711639404E-001  

Row (08) D12: +0.0000000000000000E+000  

Row (09) D21: +0.0000000000000000E+000  

Row (10) D22: -1.0000000000000000E+000  

Row (11) DG: -1.0000000000000000E+000  

-----  

INITIAL STA-TO-PCRS ALIGNMENT (R) KNOWLEDGE (1-SIGMA)  

  SIGMA(X)      SIGMA(Y)      SIGMA(Z)  

5.12250877E+000  3.95614450E-001  3.95839691E-001 [arcsec]  

-----  

PIX2RADX = 7.739989817200E-005 [rad/pixel]  

XPIXSIZE = 15.9649 [arcsec]  

PIX2RADY = 8.708614099900E-005 [rad/pixel]  

YPIXSIZE = 17.9628 [arcsec]  

CX0 = 10.5 [pixel] = 167.63 [arcsec]  

CY0 = 2.0 [pixel] = 35.93 [arcsec]  

-----  

NOMINAL BETA0 = 2.804741000000E-006 [rad/encoder unit]  

ENCODER UNIT SIZE = 0.58 [arcsec]  

GAMMA_E0 = 2007.00 [encoder unit] = 1161.09 [arcsec]  

-----  

| -1 | +0 |  

FLIP MATRIX D = |----|----| and DG = -1  

| +0 | -1 |
-----
```

### 3.3 IPF EXECUTION LOG

```

*****  

IPF EXECUTION-LOG FILE NAME: LG502087.dat  

INSTRUMENT TYPE: MIPS_160um_center_large_FOV  

IPF FILTER EXECUTION DATE: 20-Nov-2003 TIME: 18:52  

IPF FILTER VERSION USED: IPF.V3.0.OB  

*****  

----- Loading & Preparing Input Files -----  

AAFILE: AA501087 Loaded! AAFILE dimension = 290002 X 21  

ASFFILE: AS501087 Loaded!  

CAFFILE: CA902087 Loaded! CAFFILE dimension = 322 X 15  

CBFILE: CB901087 Loaded! CBFILE dimension = 178 X 15  

CCFILE: CC502087 Created! CCFILE dimension = 500 X 19  

CSFILE: CS501087 Loaded!  

Loading Input Files Completed!
-----
```

```

----- Selected Mask Vectors -----
index =  1  2  3  4  5  6  7  8  9 10 11 12 13 14 15 16 17 18 19 20
-----
mask1 = [ 0  0  0  0  0  0  0  0  0  0  0  0  0  0  0  0  0  0  0  0 ]
mask2 = [ 0  0  0  1  1  1  1  1  1  1  1  1  1  1  1  1  1  1  1  1 ]
-----

----- Selected Initial Gyro Bias Parameters -----
User Entered 1 : Use AFILE database - from S/C filter
IPF Linearized Using Following Nominal Gyro Bias Estimates
bg0 = [-4.1339711742693908E-007 -2.0063052375007828E-007 +3.6787506019209104E-007 ]
cg0 = [+0.0000000000000000E+000 +0.0000000000000000E+000 +0.0000000000000000E+000 ]
-----

----- Gyro Pre-Processor Run Completed -----
AGFILE CREATED: AG502087.m      ACFILE CREATED: AC502087.m
-----
Total Gyro Preprocessor Execution Time: 83 seconds

FRAME TABLE ENTRIES FOR PCRS LOADED TO TPCRS
q_PCRS4 = [ +5.3371888965461637E-007    q_PCRS5 = [ +7.3379987833742897E-007
            +3.7444233778550031E-004          +5.2236196154513707E-004
            -1.4253684912431913E-003          -1.4047712280184723E-003
            +9.9999891405806784E-001 ];       +9.9999887687698918E-001 ];
q_PCRS8 = [ -5.2779261998836216E-007    q_PCRS9 = [ -7.1963421681856818E-007
            +3.8462959425181312E-004          +5.3239763239987400E-004
            +1.3722087221825403E-003          +1.3516841804518383E-003
            +9.9999898455099423E-001 ];       +9.9999894475050310E-001 ];
-----

----- Initial Conditions for State ----- ----- Initial Square-Root Cov (diag) -----
p1(01) = a00 = +0.0000000000000000E+000 Sigma_initial(01,01) = 9.9999000000000000E+004
p1(02) = b00 = +0.0000000000000000E+000 Sigma_initial(02,02) = 9.9999000000000000E+004
p1(03) = c00 = +0.0000000000000000E+000 Sigma_initial(03,03) = 9.9999000000000000E+004
p1(04) = a10 = +0.0000000000000000E+000 Sigma_initial(04,04) = 9.9999000000000000E+004
p1(05) = b10 = +0.0000000000000000E+000 Sigma_initial(05,05) = 9.9999000000000000E+004
p1(06) = c10 = +0.0000000000000000E+000 Sigma_initial(06,06) = 9.9999000000000000E+004
p1(07) = d10 = +0.0000000000000000E+000 Sigma_initial(07,07) = 9.9999000000000000E+004
p1(08) = a20 = +0.0000000000000000E+000 Sigma_initial(08,08) = 9.9999000000000000E+004
p1(09) = b20 = +0.0000000000000000E+000 Sigma_initial(09,09) = 9.9999000000000000E+004
p1(10) = c20 = +0.0000000000000000E+000 Sigma_initial(10,10) = 9.9999000000000000E+004
p1(11) = d20 = +0.0000000000000000E+000 Sigma_initial(11,11) = 9.9999000000000000E+004
p1(12) = a01 = +0.0000000000000000E+000 Sigma_initial(12,12) = 9.9999000000000000E+004
p1(13) = b01 = +0.0000000000000000E+000 Sigma_initial(13,13) = 9.9999000000000000E+004
p1(14) = c01 = +0.0000000000000000E+000 Sigma_initial(14,14) = 9.9999000000000000E+004
p1(15) = d01 = +0.0000000000000000E+000 Sigma_initial(15,15) = 9.9999000000000000E+004
p1(16) = e01 = +0.0000000000000000E+000 Sigma_initial(16,16) = 9.9999000000000000E+004
p1(17) = f01 = +0.0000000000000000E+000 Sigma_initial(17,17) = 9.9999000000000000E+004
-----

p2f(01) = am1 = +0.0000000000000000E+000 Sigma_initial(18,18) = 9.9999000000000000E+004
p2f(02) = am2 = +0.0000000000000000E+000 Sigma_initial(19,19) = 9.9999000000000000E+004
p2f(03) = am3 = +1.0000000000000000E+000 Sigma_initial(20,20) = 9.9999000000000000E+004
p2f(04) = beta = +1.0000000000000000E+000 Sigma_initial(21,21) = 1.0000000000000000E-002
p2f(05) = qT1 = -1.8193149813468912E-006 Sigma_initial(22,22) = 1.0000000000000000E-002
p2f(06) = qT2 = -1.0530521324111307E-003 Sigma_initial(23,23) = 2.4834623338276731E-004
p2f(07) = aT3 = -1.7417378662919611E-003 Sigma_initial(24,24) = 1.9179929772025390E-005
p2f(08) = qT4 = +9.9999792871140569E-001 Sigma_initial(25,25) = 1.9190849786804107E-005
p2f(09) = qR1 = +7.1086635580286384E-004 Sigma_initial(26,26) = 3.6506876102645698E-005
p2f(10) = qR2 = +1.2695571640506387E-003 Sigma_initial(27,27) = 3.6506876102645698E-005
p2f(11) = qR3 = -1.6159859660547227E-004 Sigma_initial(28,28) = 3.6506876102645698E-005
p2f(12) = qR4 = +9.9999892711639404E-001
p2f(13) = brx = +0.0000000000000000E+000
p2f(14) = bry = +0.0000000000000000E+000
p2f(15) = brz = +0.0000000000000000E+000

```

```

p2f(16) = crx = +0.000000000000000E+000 Sigma_initial(29,29) = 1.3327520027739235E-009
p2f(17) = cry = +0.000000000000000E+000 Sigma_initial(30,30) = 1.3327520027739235E-009
p2f(18) = crz = +0.000000000000000E+000 Sigma_initial(31,31) = 1.3327520027739235E-009
p2f(19) = bgx = +0.000000000000000E+000 Sigma_initial(32,32) = 3.6506876102645698E-005
p2f(20) = bgy = +0.000000000000000E+000 Sigma_initial(33,33) = 3.6506876102645698E-005
p2f(21) = bgz = +0.000000000000000E+000 Sigma_initial(34,34) = 3.6506876102645698E-005
p2f(22) = cgx = +0.000000000000000E+000 Sigma_initial(35,35) = 1.3327520027739235E-009
p2f(23) = cgy = +0.000000000000000E+000 Sigma_initial(36,36) = 1.3327520027739235E-009
p2f(24) = cgz = +0.000000000000000E+000 Sigma_initial(37,37) = 1.3327520027739235E-009
-----
```

```

----- IPF KALMAN FILTER STARTED -----
Iteration#001: |dp|= +7.671596208152E-005 RMS(|Res|)=+9.582621048319E-005
Iteration#002: |dp|= +1.139240430167E-006 RMS(|Res|)=+7.967881246003E-005
Iteration#003: |dp|= +5.430186125395E-007 RMS(|Res|)=+7.968145555213E-005
Iteration#004: |dp|= +2.148726472619E-008 RMS(|Res|)=+7.968021358107E-005
Iteration#005: |dp|= +4.800143004691E-009 RMS(|Res|)=+7.968014338344E-005
Iteration#006: |dp|= +3.011242665025E-010 RMS(|Res|)=+7.968015868806E-005
Iteration#007: |dp|= +4.041571938249E-011 RMS(|Res|)=+7.968016009957E-005
Iteration#008: |dp|= +3.725349713276E-012 RMS(|Res|)=+7.968015992574E-005
Iteration#009: |dp|= +3.215485735207E-013 RMS(|Res|)=+7.968015990109E-005
Iteration#010: |dp|= +4.132345184585E-014 RMS(|Res|)=+7.968015990282E-005
Iteration#011: |dp|= +8.181675022046E-016 RMS(|Res|)=+7.968015990322E-005
Iteration#012: |dp|= +3.745976162907E-015 RMS(|Res|)=+7.968015990320E-005
Iteration#013: |dp|= +4.096016165523E-015 RMS(|Res|)=+7.968015990320E-005
Iteration#014: |dp|= +1.148126265009E-015 RMS(|Res|)=+7.968015990320E-005
Iteration#015: |dp|= +1.993803384014E-015 RMS(|Res|)=+7.968015990319E-005
Iteration#016: |dp|= +1.586417574046E-015 RMS(|Res|)=+7.968015990320E-005
Iteration#017: |dp|= +4.504009575444E-015 RMS(|Res|)=+7.968015990320E-005
Iteration#018: |dp|= +4.834464107184E-016 RMS(|Res|)=+7.968015990320E-005
Iteration#019: |dp|= +1.845140645104E-015 RMS(|Res|)=+7.968015990320E-005
Iteration#020: |dp|= +7.430471488532E-015 RMS(|Res|)=+7.968015990320E-005
Iteration#021: |dp|= +2.937264564442E-016 RMS(|Res|)=+7.968015990320E-005
Iteration#022: |dp|= +1.080753917827E-015 RMS(|Res|)=+7.968015990320E-005
Iteration#023: |dp|= +1.143894785333E-015 RMS(|Res|)=+7.968015990319E-005
Iteration#024: |dp|= +1.207712234735E-015 RMS(|Res|)=+7.968015990320E-005
Iteration#025: |dp|= +1.260564330250E-015 RMS(|Res|)=+7.968015990319E-005
Iteration#026: |dp|= +1.100578118227E-014 RMS(|Res|)=+7.968015990320E-005
Iteration#027: |dp|= +5.767527791391E-016 RMS(|Res|)=+7.968015990321E-005
Iteration#028: |dp|= +8.153927819759E-015 RMS(|Res|)=+7.968015990320E-005
Iteration#029: |dp|= +1.396429159895E-015 RMS(|Res|)=+7.968015990320E-005
Iteration#030: |dp|= +3.059546483716E-016 RMS(|Res|)=+7.968015990320E-005
IPF Kalman Filter Completed with Error |dp1| + |dp2| = +3.0595464837162876E-016
-----
```

```

----- IPF LEAST SQUARES FILTER STARTED -----
Iteration#001 COND#=+3.399419530780E+006, |dp|=+7.715544628648E-005
Iteration#002 COND#=+3.399393079514E+006, |dp|=+1.166717367825E-008
Iteration#003 COND#=+3.399393069468E+006, |dp|=+4.208309561869E-012
Iteration#004 COND#=+3.399393069462E+006, |dp|=+2.861534767028E-015
Iteration#005 COND#=+3.399393069459E+006, |dp|=+3.466718043671E-015
Iteration#006 COND#=+3.399393069463E+006, |dp|=+3.380604613106E-015
Iteration#007 COND#=+3.399393069465E+006, |dp|=+9.395259169517E-016
Iteration#008 COND#=+3.399393069460E+006, |dp|=+4.969756548831E-015
Iteration#009 COND#=+3.399393069468E+006, |dp|=+4.631949232364E-015
Iteration#010 COND#=+3.399393069458E+006, |dp|=+3.299477155652E-015
Iteration#011 COND#=+3.399393069459E+006, |dp|=+3.530822226038E-015
Iteration#012 COND#=+3.399393069460E+006, |dp|=+1.315442440000E-015
Iteration#013 COND#=+3.399393069462E+006, |dp|=+3.420048416453E-015
Iteration#014 COND#=+3.399393069466E+006, |dp|=+5.414331899546E-015
Iteration#015 COND#=+3.399393069470E+006, |dp|=+6.724515188768E-015
Iteration#016 COND#=+3.399393069465E+006, |dp|=+2.599891926036E-015
Iteration#017 COND#=+3.399393069463E+006, |dp|=+6.684267578778E-015
Iteration#018 COND#=+3.399393069462E+006, |dp|=+2.803746818403E-015
```

```

Iteration#019 COND#=+3.399393069464E+006, |dp|=+2.981902021700E-016
Iteration#020 COND#=+3.399393069468E+006, |dp|=+1.709904764621E-015
Iteration#021 COND#=+3.399393069457E+006, |dp|=+3.302392166893E-015
Iteration#022 COND#=+3.399393069466E+006, |dp|=+1.521843528315E-015
Iteration#023 COND#=+3.399393069461E+006, |dp|=+4.787473197630E-015
Iteration#024 COND#=+3.399393069465E+006, |dp|=+4.298182413357E-015
Iteration#025 COND#=+3.399393069460E+006, |dp|=+6.102854793737E-015
Iteration#026 COND#=+3.399393069472E+006, |dp|=+5.643863854450E-015
Iteration#027 COND#=+3.399393069469E+006, |dp|=+1.127192847643E-015
Iteration#028 COND#=+3.399393069464E+006, |dp|=+7.405189435630E-015
Iteration#029 COND#=+3.399393069458E+006, |dp|=+5.869985364521E-015
Iteration#030 COND#=+3.399393069457E+006, |dp|=+4.159419299094E-015
IPF Least Squares Filter Completed with Error |dp1| + |dp2| = +4.1594192990936006E-015
-----
```

Total Execution Time: 458 seconds

## 4 COMMENTS

The results of this run are summarized as follows:

1. The delivered data sets (CA501087 and CB502087) initially contained 332 MIPS science centroids and 180 PCRS centroids.
2. A 45 minute segment of attitude history data was missing in the AA file. Consequently, the first sandwich maneuver (at about 4.7 hours into the experiment) was removed because the GCF correction associated with this data was corrupted.
3. Science centroid number 149 was removed because it had a large a-posteriori prediction error. In addition, 9 science and 2 PCRS centroids were removed as part of the eliminated sandwich.
4. The MIPS team informed us, after seeing a preliminary IPF run, that there was a gross error in all of the centroids in the V direction due to uncertainties on the point spread function. For this reason, plate scales could not be reliably estimated and were not included as parameters.
5. We estimated a total of 17 parameters: 2 Brown angles for the prime frame (no Twist), 3 STA to TPF alignment, 6 thermo-mechanical induced drift, and 6 gyro drift bias parameters.
6. Plate scales were not estimated because uncertainty in the point spread function was suspected to have corrupted the V components of the science centroids. However, it was felt that the prime frame location estimates were accurate enough for FTU 14.
7. Figure 1.2 shows an inconsistency between an inferred frame in Frame Table BodyFrames\_FTU\_13Aa.x and the offset file FF502087. The MIPS instrument team informed us that it is due to the fact that this inferred frame was treated as a derived frame in an earlier Frame Table update and a small sign error was made in its calculation. The current IPF based Frame Table recommendations will solve this problem.

In summary, we recommend Frame Table changes for frames 87, 88, 89, 91 and 92 as given in the IF file IF502087.dat for FTU 14. The recommended changes are on order of: 6" in Y and 8" in Z (no Twist) for the prime frame 87. These estimates are expected to meet the fine survey pointing requirement of 3.7" (disregard the accuracies quoted in the tables). However, our confidence in these estimates is compromised by the large off-nominal centroiding errors in the V direction. Note that there are two upcoming fine survey experiments planned for FTU 15, which should be used to improve the knowledge and confidence in these frames estimates.

## IPF TEAM CONTACT INFORMATION

IPF Team email	ipf@sirtfweb.jpl.nasa.gov	
David S. Bayard	X4-8208	David.S.Bayard@jpl.nasa.gov (TEAM LEADER)
Dhemetrio Boussalis	X4-3977	boussali@grover.jpl.nasa.gov
Paul Brugarolas	X4-9243	Paul.Brugarolas@jpl.nasa.gov
Bryan H. Kang	X4-0541	Bryan.H.Kang@jpl.nasa.gov
Edward.C.Wong	X4-3053	Edward.C.Wong@jpl.nasa.gov (TASK MANAGER)

## ACKNOWLEDGEMENTS

This work was performed at the Jet Propulsion Laboratory, California Institute of Technology, under contract with the National Aeronautics and Space Administration.

## References

- [1] D.S. Bayard, B.H. Kang, *SIRTF Instrument Pointing Frame Kalman Filter Algorithm*, JPL D-Document D-24809, September 30, 2003.
- [2] B.H. Kang, D.S. Bayard, *SIRTF Instrument Pointing Frame (IPF) Software Description Document and User's Guide*, JPL D-Document D-24808, September 30, 2003.
- [3] D.S. Bayard, B.H. Kang, *SIRTF Instrument Pointing Frame (IPF) Kalman Filter Unit Test Report*, JPL D-Document D-24810, September 30, 2003.
- [4] *Space Infrared Telescope Facility In-Orbit Checkout and Science Verification Mission Plan*, JPL D-Document D-22622, 674-FE-301 Version 1.4, February 8, 2002.
- [5] *Space Infrared Telescope Facility Observatory Description Document*, Lockheed Martin LMMS/P458569, 674-SEIT-300 Version 1.2, November 1, 2002.
- [6] *SIRTF Software Interface Specification for Science Centroid INPUT Files (CAFIE, CSFILE)*, JPL SOS-SIS-2002, November 18, 2002.
- [7] *SIRTF Software Interface Specification for Inferred Frames Offset INPUT Files (OFILE)*, JPL SOS-SIS-2003, November 18, 2002.
- [8] *SIRTF Software Interface Specification for PCRS Centroid INPUT Files (CBFILE)*, JPL SIS-FES-015, November 18, 2002.
- [9] *SIRTF Software Interface Specification for Attitude INPUT Files (AFILE, ASFILE)*, JPL SIS-FES-014, January 7, 2002.
- [10] *SIRTF Software Interface Specification for IPF Filter Output Files (IFFILE, LGFILE, TARFILE)*, JPL SOS-SIS-2005, November 18, 2002.
- [11] R.J. Brown, *Focal Surface to Object Space Field of View Conversion*. Systems Engineering Report SER No. S20447-OPT-051, Ball Aerospace & Technologies Corp., November 23, 1999.